UNIVERSITÀ DI SIENA 1240

UNIVERSITA' DI SIENA

DIPARTIMENTO Di MEDICINA MOLECOLARE E DELLO SVILUPPO

DOTTORATO DI RICERCA IN
MEDICINA MOLECOLARE

CICLO XXXIII

COORDINATORE PROF. VINCENZO SORRENTINO

Allele specific silencing by RNAi of R92Q and R173W mutations in cardiac troponin T

SETTORE SCIENTIFICO-DISCIPLINARE: BIO/16

DOTTORANDO

Loredana Migliore

TUTOR

Prof.ssa Daniela Rossi

LOREDANA MIGLIORE

Firmato il 28/06/2021

ANNO ACCADEMICO: 2019/2020

Index

Abstract

Many familial forms of hypertrophic and dilated cardiomyopathy (HCM and DCM) are linked to autosomal dominant mutations in genes encoding sarcomeric proteins. Several efforts have been done to develop therapeutic approaches for these patients, including the design of Allele-Specific Silencing approaches by RNA interference (ASP-RNAi). ASP-RNAi represents a powerful and promising strategy to counteract genetic defects by using duplex small interfering RNAs (siRNAs) to target mutant alleles with minimal suppression of the corresponding wild-type allele.

We focused on the R92Q and R173W missense mutations in the cardiac Troponin T gene (cTnT) associated to HCM and DCM, respectively and developed an ASP-RNAi strategy to specifically knock-down the mutant alleles. Following siRNA design and generation, the specific silencing of the mutant allele was tested by a luciferase reporter gene assay and further confirmed on HEK293T cells expressing either the wild type or mutant cTnT alleles. siRNAs fully complementary to the target sequence or containing single-base mismatches downstream the targeted mutations were analyzed and evaluated. Results obtained showed that optimal allele discrimination was obtained with the use of siRNA containing a single-base mismatch both for the R92Q and the R173W mutations.

1. Introduction

1.1 Cardiac muscle tissue and cardiac muscle cells

Cardiac muscle tissue or myocardium is a highly organized tissue, composed of several cell types that include fibroblasts and cardiac muscle cells or cardiomyocytes. The latter are the individual functional units of cardiac muscle, providing the contractile power of the heart. Cardiomyocytes are elongated cells of cylindrical appearance, about 80 μm in length and 15 μm in diameter, characterized by a single centrally located nucleus, a branching morphology and are connect to adjacent cells through specialized sites known as intercalated discs.

Cardiac muscle tissue contracts autonomously by involuntary stimuli and it is innervated by the vegetative nervous system, which has the role of regulating the frequency of the contraction rhythm. The stimulus for contraction is produced by specialized cells of the atrial sinus node from which the electrical impulses propagate, generating the heartbeat (Monesi, 2012). The myocardium is surrounded by a connective sheath called epimysium. From this, connective tissue septa, the perimysium, depart towards the inside of the muscular structure and surround group of muscle cells. From the perimysium thinner septa depart surrounding each single myofiber, forming the endomysium, which contains capillaries and axons. A single cardiomyocyte is delimited by the plasma membrane, called sarcolemma, which surrounds and encloses the cytoplasm mass, called sarcoplasm, in which it can be found myofibrils and the cytoplasmic organelles, including an extensive specialized endoplasmic reticulum called sarcoplasmic reticulum. Myofibrils are long cylindrical structures with a diameter between 1 and 3 μm, highly specialized for contraction; the orderly arrangement of myofibrils along the major axis of the fiber gives the muscle cell the characteristic transversal striation due to the alternation of dark and light bands. Dark bands are birefringent or anisotropic, A bands, while the less dense isotropic bands are the I bands. Each I band is bisected by a darker transverse line called Z disc, while at the center of the A band there is a lighter zone called H band crossed centrally by a transverse line, the M line. The region positioned

between two Z discs represents the sarcomere, the structural and functional unit of striated muscle.

The sarcomere is composed of repeating units of thin and thick filaments, which differ in chemical composition and dimension (Figure 1). Thin filaments are composed by actin and the regulatory proteins tropomyosin and troponin, while thick filaments are composed of myosin and accessory proteins.

The myosin protein has a hexameric structure made up by two heavy chains at the C-terminal region, and four light chains forming the globular heads of the molecule, in the N-terminal region. The myosin 'head' is also called cross-bridge, since it bridges the gap between the thick myosin filaments and the thin actin filaments in muscle. Each globular head contains an ATPase domain able to hydrolyze ATP to ADP+Pi, a process required to generate the energy needed for the contraction and relaxation (Krendel M and Mooseker M, 2005). Thus, myosin structure is designed to achieve the efficient conversion of biochemical energy into force production. Another sarcomeric protein of the thick filament is Myosin Binding Protein C (MyBP-C), located in the cross-bridge containing A-band of the sarcomere, and plays a role in assembly and stability of the sarcomere as well as in the modulation of contraction (Oakley et al, 2004).

The actin protein, in turn, is composed by two twisted proto-filaments of filamentous actin (F-actin), each of which is composed by 400 molecules of globular actin (G-actin), thus resembling a row of pearls. Actin myofilaments are bound for their entire length by tropomyosin (Tm) proteins, associated head-to-tail, and by troponin (Tn) complexes regularly spaced by 40 nm on tropomyosin, which regulate the exposure of myosin binding site on actin, in a Ca^{2+} dependent mechanism (Rosol M et al, 2000). Tropomyosin of striated muscle is encoded by *TPM1* and *TPM2* genes (α and β isoforms), but only the α isoform is expressed in cardiac muscle (Perry V, 2001). The muscle shortening is associated to the reduction of width of I-band and H-zone, without any variation of A band width (Squire, 1997). So, when sarcomere shortens, reduction of the distance between neighboring Z-lines is related to the sliding of actin thin filaments towards the center of the sarcomere, causing the increase of overlapping of thin and thick filaments, without any variation in the length of both filaments (Huxley AF et al, 1954).

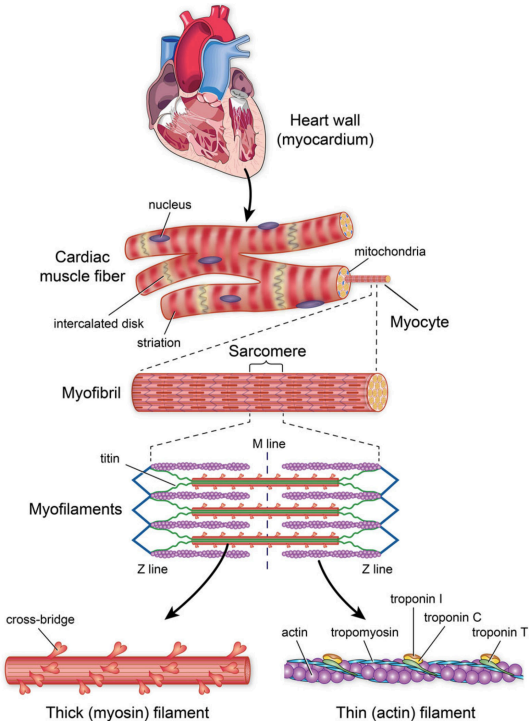

Figure 1: Cardiac muscle fiber and sarcomere structure. In the top part of the image is the myocardium, composed by cardiac muscle fibers, whose contraction allows the heart to pump blood throughout the body. Cardiomyocytes are represented as elongated cells characterized by a single centrally located nucleus, a branching morphology and the intercalated discs. Each cardiomyocyte contains myofibrils, which consist in repeating units of sarcomere, composed by thin and thick filaments. Thin filaments contain actin, tropomyosin, and troponin complex, while thick filaments are composed of myosin (Image from Golob M et al, 2014).

Two additional giant proteins, namely titin and obscurin participate in the proper organization of the sarcomeric scaffold, also contributing to mechanical and physiological properties of muscle fibers. Titin is the largest protein found in mammals (Labeit S et al, 1990) (~3800 kDa) and is anchored on both M band and Z disc with its N-terminal and C-terminal regions, respectively. On the M band, titin interacts with obscurin and myomesin, contributing to M band stability, while it binds to obscurin and α-actinin on Z disc (Gautel M et al, 2016). As a consequence, two molecules of titin generate a protein backbone that spans along the entire sarcomere length. Obscurin (850 kDa) is a sarcomeric protein mainly present at the M band and at a lesser extent at Z disc and it is involved in ankyrinB-dependent dystrophin localization and overall sarcolemma integrity

(Randazzo D et al, 2013). It has been also reported that Obscurin interacts with a muscle-specific protein localized in the SR, namely small ankyrin 1.5 (sAnk1.5); this association is responsible for the proper positioning of the SR around myofibrils (Bagnato P et al, 2003; Armani A et al, 2006; Lange S. et al, 2009).

Nebulette (109 kDa) is a cardiac-specific isoform belonging to the nebulin family and it is exclusively localized in the Z-disc where it is involved in structure stability and contractile performance (Pappas et al, 2011).

Dystrophin (427 kDa) is localized in correspondence of the Z disc and is part of a protein complex called Dystrophin Glycoprotein Complex (DGC). This structure is the core of costamere, a multi-protein complex of the sarcolemma localized in correspondence of the Z-discs. This complex acts as a bridge between fiber actin cytoskeleton and the extracellular matrix, in order to dissipate the mechanical stress generated by repeated cycles of contraction and to protect the integrity of the sarcolemma (Ervasti JM, 2003).

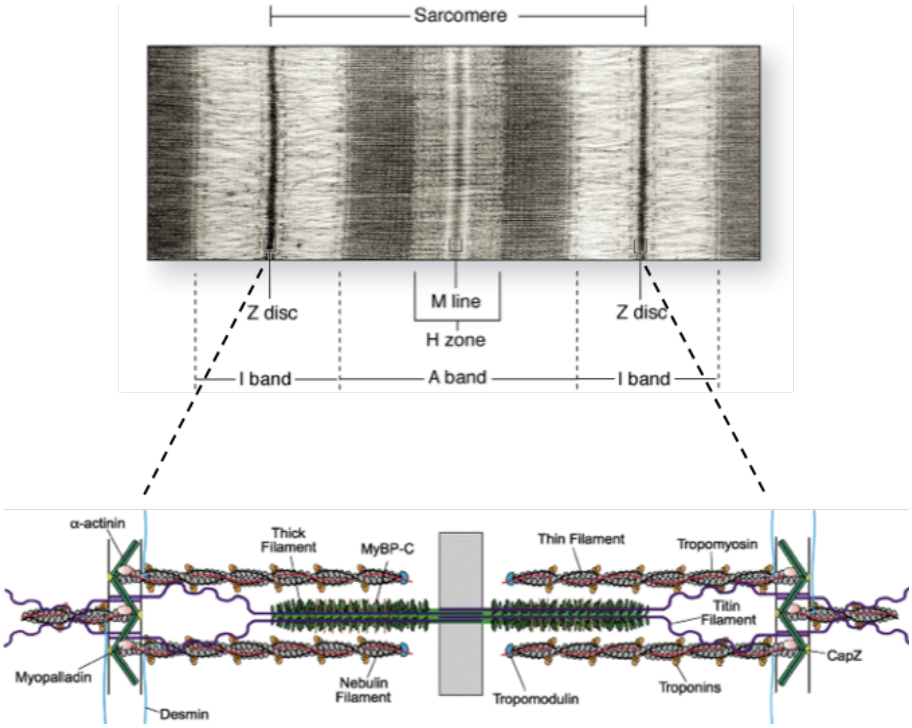

Figure 2: Localization of cardiac sarcomere proteins. Electron micrograph of striated muscle in longitudinal section, showing one sarcomere. On each side of the Z disc are the lightly stained I bands, composed of actin thin filaments. The H zone, which

is made up exclusively of myosin thick filaments, is in the center of the A band that includes a zone of overlap between the thick and thin filaments (Image on top from Junqueira and Carneiro, 2005; figure on the bottom adapted from McElhinny et al, 2003).

1.2 The Troponin complex

The Troponin complex is a heterotrimeric complex identified as the regulatory unit of the thin filament (Ebashi S et al, 1967). Tn is the Ca^{2+} regulator of striated muscle contraction and is composed of three subunits which interact strongly with one another: cardiac Troponin C (cTnC) the Ca^{2+} binding subunit, Troponin I (cTnI) the inhibitory subunit and troponin T (cTnT) the tropomyosin binding subunit (Gomes AV et al, 2002). Each Tn complex is associated to one Tm molecule and both bind to seven G-actin monomers (Parmacek MS. and Solaro J, 2004).

The main role of the Tn complex is to regulate the motor function of the actomyosin complex following a change in intracellular calcium concentration. In diastole, at low Ca^{2+} concentration, the N-terminal domain of TnC (N-TnC) containing the Ca^{2+} specific binding site, known as the 'regulatory head' of Tn (Figure 3B), is empty. The C-terminal domain of TnC (C-TnC) is bound to the N-TnI, as well to the globular C-TnT. Troponin complex docks to the thin filament by the link of N-TnT to tropomyosin and by the link of both the C-TnI and the TnI inhibitory peptide (Ip) to actin, maintaining the thin filament in a conformation that inhibits the actomyosin interaction. In systole, Ca^{2+} binds to the Ca^{2+} specific site of N-TnC inducing the increase of this domain's affinity both for the N-TnI, that occurs when Ser23/Ser24 of N-TnI are unphosphorylated, and for the switch peptide (Sp) of TnI, resulting in the release of Ip from actin. Consequently, tropomyosin shifts in a new position on the actin filament leading to the actomyosin interaction and to muscle contraction (Figure 3A) (Parmacek MS. and Solaro J, 2004). The ATPase domains of myosin heads hydrolyze ATP, producing the energy required for myosin movement and sarcomere shortening. Myosin flexes of nearly 45° pulling the actin filament of

about 10 nm in the direction of the M band. As a consequence, during contraction sarcomeres shorten, and the width of the I-bands is reduced due to the sliding of thin filaments on thick filaments. To ensure an immediate subsequent new contraction cycle ADP unbinds, and a new ATP molecule binds to myosin heads, thus unfastening myosin from the actin filaments. The hydrolysis of new ATP in ADP+Pi initiates a new cycle of contraction.

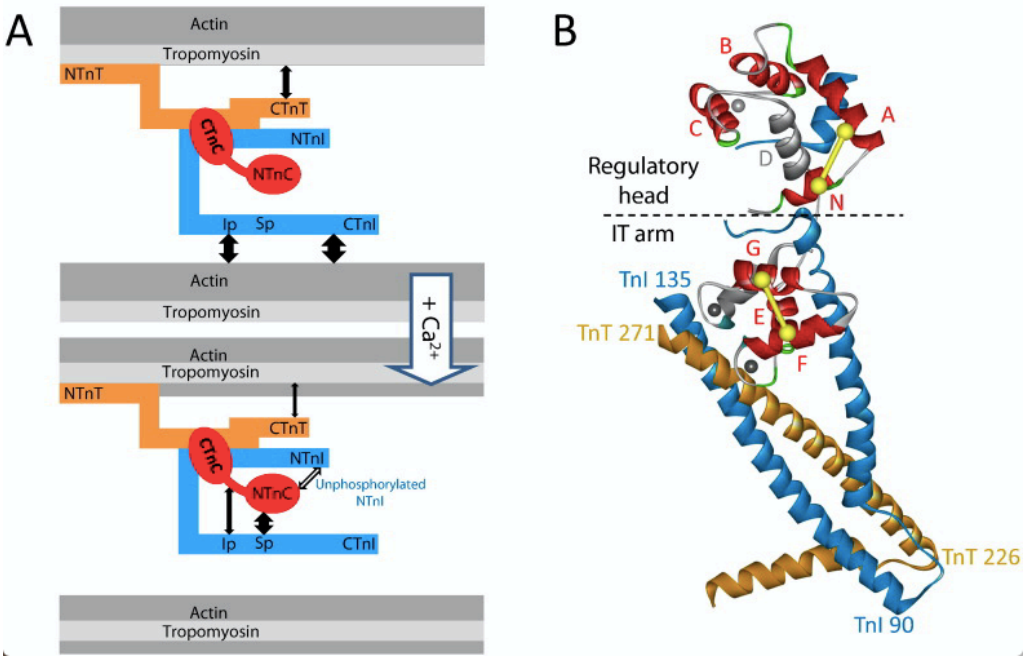

Figure 3. The interaction between the components of cardiac thin filament (A) and structure of troponin complex (B): Panel A is a schematic representation of the Ca^{2+} dependent interactions between Tn complex, Tm and actin. Ip, TnI inhibitory peptide; Sp, TnI switch peptide. The interaction between cardiac specific N-TnI and N-TnC in the presence of Ca^{2+} occurs when Ser23/Ser24 of N-TnI are unphosphorylated. Panel B shows the structure of cardiac Tn complex. TnT is in yellow, TnC in red and TcI in blue. The 'regulatory head' of Tn is the N-terminal domain of the TnC (N-TnC) which contains the regulatory Ca^{2+} binding site. The 'IT-arm' is a rigid domain containing a long coiled-coil formed by helices from TnI and TnT, plus the C-terminal domain of TnC (C-TnC) (Image from Sevrieva I et al, 2014).

TnI is a 24 kDa protein responsible for inhibiting the activity of the actomyosin ATPase and holding the troponin complex bound to actin. Three isoforms of TnI, encoded by three different genes are present in mammals: fast skeletal

troponin I (*TNNI2*), slow skeletal troponin I (*TNNI1*) and cardiac troponin I (*TNNI3*).

Cardiac troponin I (cTnI) consists of five domains: N-terminal, IT-arm, inhibitory peptide (Ip), regulatory domain, and C-terminal mobile domain. The N-terminal domain is present exclusively in the cardiac isoform of TnI and plays a crucial role in the interaction between cTnI and cTnC and in the regulation of muscle contraction. The acidic N-terminal domain of cTnI binds the N-terminus of cTnC, but the phosphorylation of cTnI at the PKA sites Ser23 and Ser24 of N-terminal domain leads to a decrease in myofilament Ca^{2+} sensitivity through a conformational change of the troponin complex. This structural change reduces the affinity of Ca^{2+} binding to cTnC (Howarth JW et al, 2007; Zhang R et al, 1995). The IT-arm, a rigid domain (amino acid residues 40-136 in humans), is composed of two alfa helices (H1 and H2), connected by a short linker which interact with cTnC and cTnT, respectively. The inhibitory domain (amino acid residues 137-146 in humans) of cTnI is considered to be responsible to inhibition of the interaction between actin and myosin by binding actin at low Ca^{2+} concentration (Sadayappan S et al, 2008). The regulatory domain (amino acid residues 164-210 in humans) of cTnI is the second actin-Tm binding site and includes a short alfa helix that, at high Ca^{2+} concentrations, interacts with the N-terminal domain TnC (Li MX et al,1999; Katrukha IA, 2013).

TnC is the Ca^{2+}-binding subunit of the Tn complex and its interaction with TnI and TnT is central to the regulation of skeletal and cardiac muscle contraction.

TnC is an 18.4 kDa protein encoded in humans by two different genes: one gene, *TNNC2,* is expressed in fast skeletal muscle, while the second gene is expressed in both cardiac and slow skeletal muscle (*TNNC1*) (Zot AS et al, 1987). cTnC consists of a short N-terminal regulatory domain and a C-terminal structural domain connected by an alpha helical linker (Slupsky & Sykes, 1995). Each domain consists of EF hand helix-loop-helix motifs as Ca^{2+}-binding sites (Kretsinger RH, 1980). Specifically, the C-terminal domain of cTnC contains two high-affinity sites for Ca^{2+} that are always occupied by Ca^{2+} or Mg^{2+}, while the N-terminal domain has only one low-affinity Ca^{2+} binding site that is largely unoccupied at resting calcium concentrations (Potter JD and Gergely J, 1975).

The activation of cardiac muscle contraction occurs when Ca^{2+} binding to the N-terminal domain of cTnC induces an open conformation that binds to the switch region of cTnI, removing adjacent inhibitory regions of cTnI from actin and allowing the trigger of muscle contraction (Li M et al, 2015).

Troponin T (TnT) is the largest troponin subunit and a central player in the cardiac contraction mechanism in response to the calcium concentration surrounding the contractile apparatus (Perry SV, 1998). Troponin T is expressed in humans by three genes encoding slow, fast skeletal and cardiac (TNNT1, TNNT3, TNNT2) isoforms of the protein. The cardiac troponin T gene (*TNNT2*) is located on chromosome 1 (1q32.3), is 17 kb long and consists of 17 exons and 16 introns (Mesnard L et al, 1995; Townsend PJ et al, 1994; Farza H et al, 1998). It encodes a protein of 33 kDa. TNNT2 is subjected to substantial alternative splicing of exons 4, 5 and 13, which leads to the expression of several cTnT isoforms (Mesnard L et al, 1995; Townsend PJ et al, 1994; Anderson PA et al, 1991). The exon 5 is spliced in the cTnT in adult heart and is expressed only in the embryonic form of cTnT (Sabry MA, 1989; Anderson PA et al, 1991). Exons 4 and 13 are alternatively spliced during all developmental stages (Anderson PA et al, 1995). The exact time of disappearance of human embryonic cardiac TnT expression is not known, but by the ninth month of postnatal development embryonic TnT is completely substituted by the adult form (Townsend PJ et al, 1994). In the heart of healthy adults, troponin T is mainly present as isoform 3, which is 287aa long and incorporates the amino acid sequences coded by exons 4 and 13 (Anderson PA et al, 1995).

cTnT plays a crucial role in anchoring the cTn complex to the thin filament by interacting with Tm. Structurally, cTnT contains two functional domains: N-terminal domain (amino acid residues 2-67) and C-terminal domain (amino acid residues 201-288) separated by a central region and a flexible linker region (amino acid residues 68-182 and 183-200, respectively) (Figure 4) (Ohtsuki I, 1979; Wei B and Jin JP, 2011). The N-terminal domain modulates the conformation and function of cTnT and affects the calcium sensitivity of the muscle and the development of the maximal force of the contraction. The central region binds to the head-tail junction of Tm independently of Ca^{2+} concentration.

The C-terminal domain contains α-helices H1 (residues 204-220) and H2 (residues 226-271), which are responsible to link cTnI and cTnC and it also contains a second site of interaction with tropomyosin in a Ca^{2+} sensitive manner (Katrukha IA, 2013; Takeda S et al, 2003).

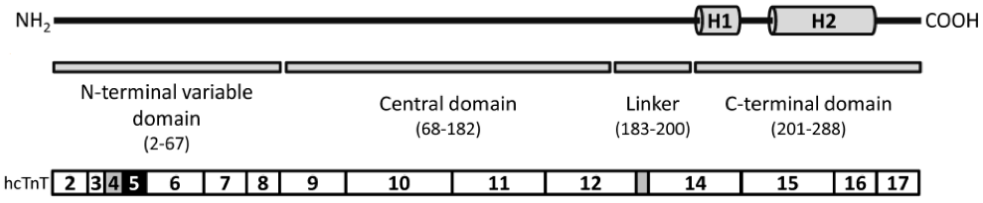

Figure 4. Human cardiac troponin T protein domains and *TNNT2* exons

(Image from Katrukha IA, 2013)

1.3 Sarcoplasmic reticulum, T-tubule and dyad

The Sarcoplasmic Reticulum (SR) is a specialized form of Endoplasmic Reticulum (ER) dedicated to calcium storage and release in order to activate muscle contraction. SR consists of two morphologically and functionally distinct domains: the longitudinal SR (l-SR), specialized in calcium up-take, and the junctional SR (j-SR), which regulates calcium release. The l-SR is composed of a network of parallel tubules oriented longitudinally along the major axis of the fiber. L-SR is the main site for Ca^{2+} storage and uptake from the cytosol, a process depending from the SR/ER Ca^{2+} ATPase (SERCA) pumps. The longitudinal tubules end into dilated sacs, the terminal cisternae or j-SR, oriented in the transversal direction (Rossi D et al, 2008).

Specific of striated muscle cells, T-tubule is an invagination of the sarcolemma, penetrating into the intracellular space of myocytes. In cardiomyocytes, T-tubule is a large structure that wraps around the Z disc forming a specialized structure with a terminal cisterna, knows as dyad, the site of Excitation-Contraction Coupling (ECC) in the cardiac muscle (Figure 5) (Hong et Shaw, 2017).

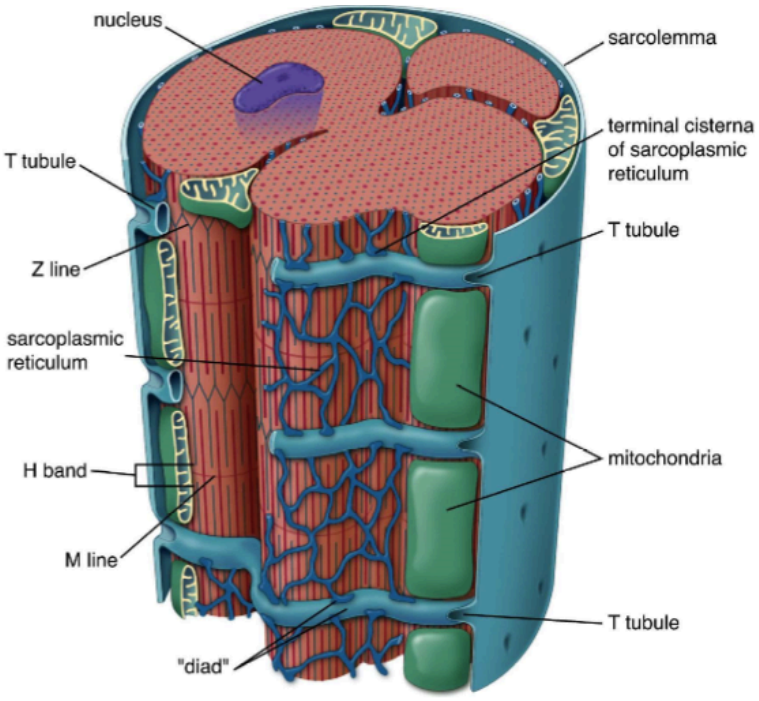

Figure 5. Sarcoplasmic reticulum and dyad structure
(Image from Ross & Pawlina, 2016)

1.3.1 Cardiac Excitation-Contraction coupling (ECC)

ECC involves a close interplay between type 2 ryanodine receptors (RyR2) with cardiac L-type voltage-gated Ca^{2+} channels (Cav1.2) within the dyadic space (Scriven et al, 2013). ECC is a sequence of events that, from a nervous stimulus, leads to the muscle contraction (Sandow, 1965). In myocardium the contractile impulse originates autonomously; the sinoatrial node cells spontaneously produce an action potential that travels along the sarcolemma flowing from a cardiomyocyte to the next. When an action potential reaches the T-tubule system results in the activation of voltage-sensitive L-type Ca^{2+} channels (Cav1.2). The rapid but small influx of calcium though the Cav1.2 causes activation of RyR2 Ca^{2+} release channels on the j-SR, resulting in the release of a larger amount of calcium into the cytosol, a mechanism called Ca^{2+}-induced Ca^{2+} release (CICR) (Balke CW et al, 1998).

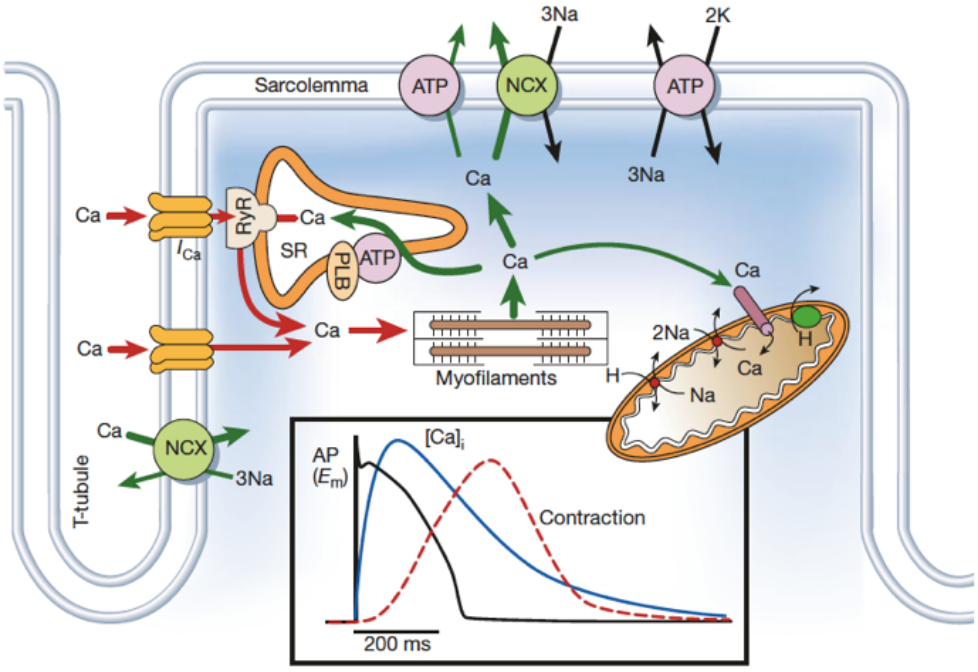

Figure 6. Ca^{2+}-induced Ca^{2+} release (CICR) mechanism. Ca^{2+} transport of ventricular myocytes. NCX, Na^+/Ca^{2+} exchange; ATP, ATPase; PLB, phospholamban; SR, sarcoplasmic reticulum (Image from Bers DM; 2002).

The increase in cytosolic calcium allows the binding of calcium to troponin C, resulting in elimination of the inhibition imposed by troponin I and tropomyosin on the actin-myosin interaction, inducing the thin filaments to slide over the thick ones, thus producing contraction (Craig R et al, 2004).

To induce relaxation at the end of contraction, resting calcium must be removed from the cytosol. The restore of Ca^{2+} is provided by the action of Ca^{2+} pumps, represented by SERCA, sarcolemmal Na^+/Ca^{2+} exchanger, sarcolemma Ca^{2+}-ATPase (PMCA) and mitochondrial Ca^{2+} uniport (Bers DM, 2002).

1.4 Cardiomyopathies

Cardiomyopathies (CMPs) are myocardial disorders characterized by structural and functional abnormalities in the heart muscle (Braunwald E et al, 2017). In 1957 the term cardiomyopathies was used for the first time to describe a group of uncommon myocardial diseases (Brigden W, 1957). Later, in 1960, the cardiologist Goodwin defined CMPs as 'myocardial disease of unknown cause' and identified three different entities, called hypertrophic CMP (HCM), dilated CMP (DCM) and restrictive CMP (RCM) (Goodwin JF et al, 1961). A few years later other elements in the classification were added, such as arrhythmogenic right ventricular cardiomyopathy (ARCV) and left ventricular noncompaction (LVNC). Classification of CMPs was revisited during the years. Nevertheless, it was maintained a distinction between primary CMPs, when disease is predominantly of the heart muscle, and secondary CMPs, when myocardial involvement is associated with a multisystem disorder. In addition, primary CMPs were classified as genetic (HCM, ARVC, LVNC), acquired (peripartum, tachycardia induced, myocarditis), or mixed (DCM, RCM) (Elliott P et al, 2008). The most recent classification of CMPs is proposed by the World Heart Federation in 2013, known as the MOGE(S) classification, that includes both genotype and phenotype features (Arbustini E et al, 2013).

HCM is the most common subtype with a prevalence of 1 to 500 (Maron BJ et al, 1995; Frisso G et al, 2009). The HCM is characterized by left ventricular hypertrophy with wall thickness more than 1.5 cm larger than the normal size (Figure 7C) in the absence of other cardiac or systemic disease (Masarone D et al, 2018; Maron BJ et al, 2013). Phenotypic expression is variable, and some patients with HCM have a normal life expectancy with minimal or no disability (Gersh B et al, 2011). Many patients with HCM are asymptomatic and are diagnosed during family screening. The functional changes in HCM are hyperdynamic contraction, progressive diastolic dysfunction of the cardiac ventricles and increased energy consumption. The most characteristic symptoms of HCM include atypical chest pain, dyspnea, palpitations, atrial fibrillation with risk of progressive development of heart failure and sudden cardiac death (Fifer

MA et al, 2008). The main causes of sudden death are primary ventricular tachycardia and ventricular fibrillation. Heart failure is characterized by preserved left ventricular systolic function and is more frequent in middle-aged adults. In this case, it is recognized a difference by sex, in which women have more severe symptoms than men. Other determinants of heart failure in HCM patients include left ventricular outflow-obstruction, atrial fibrillation and diastolic function (Maron BJ et al, 2012).

DCM prevalence is 1 to 2500 (Bozkurt B et al, 2016). It is defined by enlargement of ventricles, normal left ventricular wall thickness and systolic dysfunction (Figure 7B) (Mathew T et al, 2017). Approximately 25% to 35% of cases are familial with an autosomal dominant pattern, caused by mutations in cytoskeletal, sarcomeric or intercalated disc proteins. Examples of acquired causes of DCM include myocarditis, neuromuscular disorders, nutritional deficiencies, endocrine dysfunction and the administration of cardiotoxic drug and viral infectious (Luk A et al, 2009; Hsu DT et al, 2010). DCM can occur at any age but, most commonly, it occurs in the third or fourth decade of life (Dec GW and Fuster V, 1994). The characteristic symptoms are arrhythmias, thromboembolic events (Masarone D et al, 2018). DCM is the third most common cause of heart failure (Towbin JA et al, 2006).

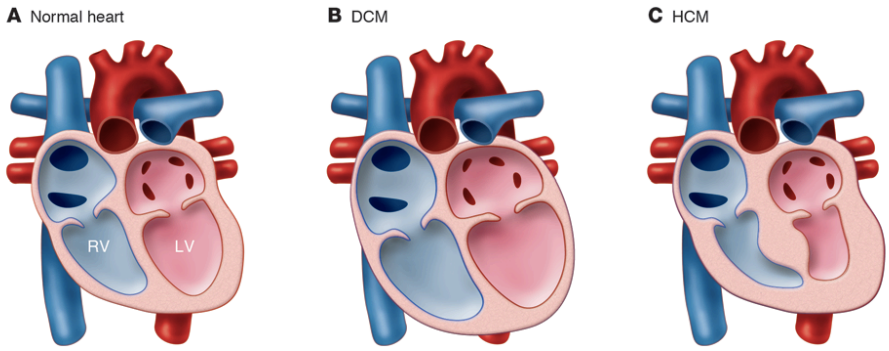

Figure 7. Morphological changes to the heart in cardiomyopathy. (A) Normal heart. **(B)** In DCM, the heart enlarges with increased diameter and reduced function. **(C)** In HCM, the myocardium especially in the Left Ventricle becomes thicken, leading to impaired filling and emptying (Image from McNally E et al, 2013).

RCM is defined by restrictive ventricular physiology in the presence of normal or reduced diastolic volumes of one or both ventricles, normal or reduced systolic volumes, and normal ventricular wall thickness (Muchtar E et al, 2017). The symptoms are pulmonary congestion and mitral regurgitation, hepatomegaly, ascites and tricuspid regurgitation (Nihoyaynnopoulos P et al, 2009). Atrial fibrillation is also common as well as normal ventricular dimension but grossly enlarged atria (Masarone D et al, 2018).

Arrhythmogenic Right Ventricular Cardiomyopathy (ARVC) has a prevalence of 1:1000 to 5000; it is an inherited disease of desmosomal proteins. ARVC is characterized by fibrofatty infiltration of healthy myocardium leading to thinning and ballooning of the ventricular wall. It's most commonly presents in the fourth decade of life with symptoms such as palpitations, syncope, and, occasionally, sudden cardiac death (Basso C et al, 2009).

Left Ventricular Noncompaction (LVNC) is an uncommon and recently identified congenital cardiomyopathy, a condition of embryonic origin that interferes with the development of mature heart muscle (Maron BJ et al, 2006). The disease lead to left ventricle dysfunction and to heart failure, arrhythmias, thromboembolic events and sudden cardiac death (Ikeda U et al, 2015).

1.4.1 Mutations linked to hypertrophic and dilated cardiomyopathy

Currently, more than 1400 mutations have been identified in HCM, mostly represented by dominant mutations in genes encoding thick and thin contractile myofilament protein components of the cardiac sarcomere (Van der Velden J et al, 2017). About the 70% of these mutations occur in β-myosin heavy chain (*MYH7*) and myosin binding protein C (*MYBPC3*), while 1% to 5% or less are present in Troponin T (*TNNT2*), Troponin I (*TNNI*), α-tropomyosin (*TPM1*), α-actin (*ACTC1*), myosin light chains (*MYL3*) (Seidman CE et al, 2011). The vast majority of pathogenic mutations altering physical and functional properties of proteins are missense, frameshift mutations often resulting in a shortened

truncated protein or abnormal spicing of messenger ribonucleic acid (mRNA) (Maron BJ et al, 2012).

All HCM mutations identified in *MYH7* gene are missense mutations (R403Q, R403Q, R453C, R719Q, R719W, L908V) that act in a dominant negative manner through incorporation of the mutated protein into the sarcomere. In contrast, most *MYBPC3* mutations (VS17 + 4A > T truncated at 868; c.2864_2865delCT truncated at 860) generate a C-terminal truncated protein; therefore, the *MYBPC3* mutations are predicted to cause haploinsufficiency (Marston S. et al, 2009; van Dijk SJ et al, 2009). Heterozygous *MyBPC3* null mice carrying only one functional allele show a slight decrease in *MYBPC3* expression and a late-onset hypertrophy phenotype, consistent with a haploinsufficiency mechanism (Carrier L et al, 2004 Kulikovskaya I et al, 2003). MYH7 missense variants and MYBPC3 truncated proteins destabilize the myosin interacting-heads motif and this results in a state in which myosin can more readily interact with actin and utilize ATP inducing an increase of contractility and energy consumption (Toepfer CN et al, 2019).

Ca^{2+} sensitization in cardiac muscle contractility is a common effect caused by HCM-linked *TNNI* and *TNNT2* mutations. R145G, R145Q, R162W, ΔK183 and K206Q mutations in *TNNI*, as well as F110I and E244D mutations in *TNNT2*, significantly increase the Ca^{2+} sensitivity of myofibrils, suggesting a common mechanism in the pathogenesis of HCM (Yanaga F. et al, 1999; Takahashi-Yanaga F. et al, 2000). R162W mutation in *TNNI* was also found to affect the cTnI-cTnC protein interaction (Takahashi-Yanaga, F; 2001). HCM-mutations in α-tropomyosin (*TPM1*), like E180G and D175N lay within a region that has been implicated in the binding of the C-terminus of cTnT (Malnic B. et al, 1998), (Marston SB, 2011).

Dilated cardiomyopathy (DCM) is far more genetically heterogeneous, with mutations in genes encoding sarcomeric, cytoskeletal, and regulatory proteins: the cardiac a-actin (*ACTC*), desmin (*DES*), d-sarcoglycan (*SCGD*), vinculin (*VCL*), titin (*TTN*), T troponin (*TNNT2*), a-tropomyosin (*TPM1*), muscle LIM protein (*MLP*), phospholamban (*PLN*), ZASP (*LDB3*), and b-myosin heavy

chain (*MYH7*) (Gerull B et al, 2002; Knoll R et al, 2002; Kamisago M. et al, 2000).

MYH7, TNNT2 and *TPM1* are the most frequent mutated sarcomere genes in DCM, ranging from approximately 2 to 4%, of diagnosed DCM, while *MYBPC3* mutations are rare (Pugh TJ et al, 2014).

A total of 11 missense mutations have been found in *MYH7* as a cause of DCM (Morimoto S, 2008). The S532P mutation in *MYH7* gene occurs in the actin binding domain reducing the force-generating capacity and the velocity of actin filament sliding. The F764L mutation in *MYH7* gene occurs in the ATPase domain reducing only the actin-activated ATPase activity (McNally E et al, 2013; Schmitt JP et al, 2006).

Frameshift and nonsense mutations or predicted splice site in *TTN* gene alter the titin structure resulting in a truncated protein (Herman DS et al, 2012). The V154M mutation in *TTN* gene decreases the affinity of titin Z1-Z2 domains for T-cap, as well as the affinity of the titin Z-repeat region for a-actinin by the A743V mutation causing DCM (Itoh-Satoh M et al, 2002).

E40K, E54K and D230N missense mutations have been identified in the *TPM1* gene as a cause of DCM with a relatively malignant phenotype and all three mutations decrease the Ca^{2+} sensitivity (Chang AN et al, 2015; Lakdawala NK, 2010). Also the missense mutation G159D in *TNNC* results in a lower Ca^{2+} sensitivity, correlated with lower Ca^{2+} affinity for TnC (Robinson P. et al, 2007), a lower rate of cross-bridge turnover and sometimes, lower cooperativity. Therefore, the DCM mutations produce a hypocontractile molecular phenotype, the opposite of HCM mutations (Mogensen J et al, 2004; Mirza M et al, 2005).

1.4.2 Cardiac troponin T mutations in cardiomyopathies

Mutations in *TNNT2* gene account for approximately 1-5% of familial HCM cases (Wei B and Jin JP; 2016). At least 52-point mutations of *TNNT2* have been reported to cause human heart diseases, including 50 missense mutations, one deletion and one splicing donor site mutation (Willott RH et al, 2010).

Disease-causing mutations in cTnT are highly clustered within two primary locations, central and C-terminal regions of the protein. Approximately 65% of

the *TNNT2* mutation, most of them HCM-linked, are found between exons 9 to 12 and in exons 16 and 17, corresponding to the tropomyosin-binding domain of TNNT2. Therefore, these mutations may alter the flexibility of the domain, that is necessary for the transduction of Ca^{2+} activated signal (Manning et al, 2012). Most of the DCM-linked mutations occur in exon 11 and between exons 14 and 16, involved in binding to complex Tn proteins (Figure 8). Thus, the mechanisms involved in the pathogenesis of cardiomyopathies triggered by mutations in *TNNT2* include alteration of the Ca^{2+} sensitivity of troponin complex and changes in the binding affinity of cTnT to cTnI and cTnC (Harada and Potter, 2004).

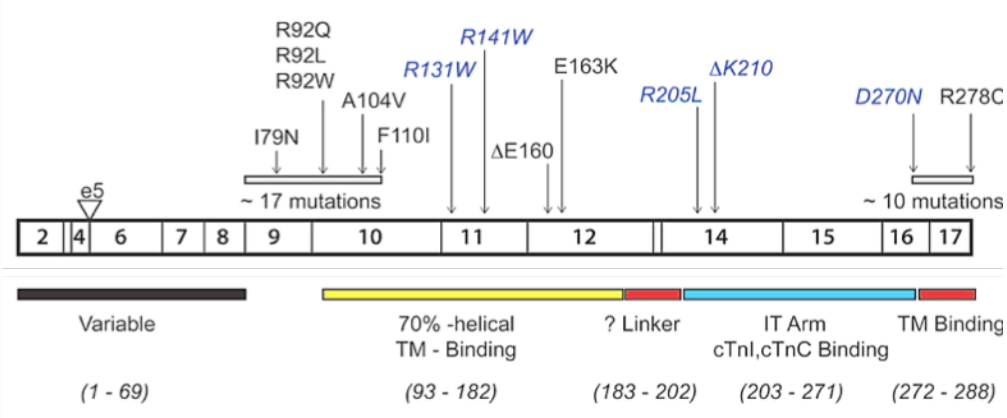

Figure 8. Distribution of HCM and DCM linked mutation in cTnT gene: Human cTnT exons, structure and functional domains. DCM-causing mutations are shown in blue, HCM-causing mutations in black (Image from Tardiff JC et al, 2011).

Missense mutations identified as cause of HCM include R92Q, I79N (Morimoto S. et al; 1998; Schwartz K and Mercadier JJ, 2003), R92L, R94L (Palm T et al, 2001). E244D (Nakaura H et al, 1999; Harada K and Potter JD, 2004), K273O (Fujino N et al, 2002) and R278C mutations (Theopistou A et al, 2004) in the C-terminal region of cardiac *TNNT2* increase calcium sensitivity and cause dominantly inherited HCM.

R92Q and Δ160E are consistently associated with a particularly poor clinical prognosis (Alcalai R et al, 2008). Mutations at R92 site of *TNNT2* are linked with a high risk of lethal arrhythmias in adolescents and young adults (Ferrantini

C et al, 2017). It's to note that these mutations are located in the middle region of *TNNT2,* resulting in decrease of cooperativity with tropomyosin and in increase in calcium sensitivity (McConnell M et al, 2017).

R92Q mutation has been extensively characterized in transgenic mouse models. HCM mouse model carrying the R92Q mutation presents excitation-contraction coupling alterations that slowed down the Ca^{2+} transient, exhibiting diastolic dysfunction and increase arrhythmogenicity (Ferrantini C et al, 2017). These mice show cardiac myocyte disarray, increased myocardial interstitial collagen content and diastolic dysfunction. The observed phenotypes are virtually identical to HCM phenotypes in humans (Oberst L et al, 1999). Isolated cardiac myocytes from R92Q mice have increased basal sarcomeric activation, impaired relaxation and shorter sarcomere length. Independent studies showed consistent results reporting hypercontractility and diastolic dysfunction, both of which are common findings in patients with HCM (Tardiff JC et al, 1999). Transgenic mice over-expressing *TNNT2*-I79N show an increase of myofilament calcium sensitivity, diastolic malfunction and increased susceptibility to arrhythmia (Baudenbacher F et al, 2008).

TNNT2 mutations causing DCM were also found in both central and C-terminal regions of *TNNT2* gene. For example, single residue deletion of K210 (Kamisago M et al, 2000), R141W (Li d. et al, 2001), R205L, R131W and D270N mutations (Mogensen J et al, 2004) are located in the central region of *TNNT2* and are found to reduce Ca^{2+} sensitivity and cause dilated cardiomyopathy.

R173W in *TNNT2* is localized in the middle region of *TNNT2* and it has been identified in multiple families. It causes decreased calcium sensitivity in the myofilaments and consequent decreased contractility (Morimoto S, 2007; Hershberger RE et al, 2009).

Sun *et al.* generated induced pluripotent stem cells (iPS) from a DCM patient with the R173W variant and demonstrated sarcomeric disorganization, depressed contractility, altered calcium ion regulation, impaired contractility and increased susceptibility to inotropic stress (Sun N et al, 2012). Localized in the C-terminal region of *TNNT2*, in the cTnT-cTnI interacting region, the E244D

(Tobacman LS et al, 1999), K247R, D270N, N271I and K273E mutations result in disruption of the stability of Tn complex.

Mutation	Mutation type	Cardiomyopathy	Ca^{2+} sensitivity
R92Q	Missense	HCM	Increased
R92L			
R92W			
R94L			
E244D			
K273O			
R278C			
I79N			
A104V			
F110L			
E163K			
ΔE160	Deletion		
c.821+1G>C	splicing donor site		
R141W	Missense	DCM	Decreased
R205L			
R131W			
D270N			
R173W			
E244D			
K247R			
N271I			
K273E			
ΔK210	Deletion		

Table 1. Summary of HCM and DCM linked mutation in *TNNT2* gene

It should be noted that some *TNNT2* mutations have been reported to be associated with clinical phenotypes of more than one type of cardiomyopathy. Moreover, it's interesting to note that no mutation has been found in the N-terminal domain of cTnT, corresponding to the hypervariable region of cTnT, which is naturally tolerant to structural variations (Wei and Jin, 2011).

1.5 Gene Therapy

Gene therapy encloses several approaches to treat hereditary and acquired diseases by manipulation of genetic material, replacing a mutated gene with the healthy gene or editing a mutated gene (Verma IM. et al, 2000). The first trial of human gene therapy has been approved in 2004 for heart failure (Jaski BE et al, 2009) and to date, the number of clinical trials investigating gene therapies is increasing worldwide (Hanna E et al, 2017).

Different strategies have been adopted in gene therapy, including genome editing, exon skipping, spliceosome-mediated RNA trans-splicing, allele specific silencing and gene replacement therapy. Concerning cardiomyopathies, treatments focus on symptoms relief by pharmacological intervention and prevention of sudden cardiac death. Several therapeutic approaches have been devised to prevent cardiomyopathies development, correcting the mutation before the beginning of symptoms (Repetti GG et al, 2019).

In genome editing, a double-strand break is created using engineered nucleases that modify the genome in a site-specific manner. The CRIPSR technique was developed enabling editing of a target-specific DNA sequences of the genome using a nuclease (Cas9), responsible for cleavage of the double-strand DNA based on the use of an RNA guide, which is complementary to the genetic locus of interest (Jinek M et al, 2012). CRISP/Cas9 was successfully used for the generation of HCM and genetic correction of HCM induced pluripotent stem cells (iPSC). The I79N mutation in *TNNT2* gene was introduced into hiPSCs by use of CRISP/Cas9, reproducing an HCM model with myofilament disarray, hypercontractility and diastolic dysfunction (Wang L et al, 2017). In *PRKAG2*-mutated iPSC-CMs, CRISP/Cas9 correction eliminated the functional and structural defects, electrophysiological abnormalities and cardiomyocyte hypertrophy (Ben Jehuda R et al, 2018). In addition, CRISPR/Cas9 has been used to correct an HCM pathogenic mutation in the *MYBPC3* gene (Ma H et al, 2017).

In the RNA trans-splicing methodology, an exogenous RNA is introduced into the target cell, usually by means of gene transfer, to induce a splice event in trans between the exogenous RNA and the target endogenous pre-mRNA. The result is a chimeric mRNA composed partly of exons of the latter, and partly of exons of the former, encoding a sequence free of mutations.

In the contest of HCM, RNA-trans splicing was tested in both iPSC-CM carrying the *Mybpc3* mutation and in vivo in *Mybpc3* targeted knock-in mice; however, a very low trans-splicing efficiency was observed with no restoration of the cMyBPC3 protein (Mearini G et al, 2013; Prondzynski M et al, 2017). These studies showed that further optimization is needed to increase trans-splicing efficiencies, so that it can be taken into consideration as a treatment option in humans.

Gene replacement therapy is mainly applied when a mutation results in a low level or absence of the corresponding protein. The full-length wild-type cDNA of the target gene is delivered by a vector into the cell or by a viral system, such as Adenovirus associated virus (AAV) (Prondzynski M. et al, 2018). AAV9 used to deliver full length wild-type *Mybpc3* cDNA in *Mybpc3* knock-in mice prevents the development of cardiac hypertrophy and dysfunction by increasing the amount of cMyBPC3 protein (Mearini G et al, 2013).

Rapid development in allele-specific silencing by RNA interference (ASP-RNAi) has proven to be another option to cure autosomal dominant diseases by targeting the mutant allele. Therapeutic benefit has been demonstrated in iPSC-CM from patients and in mouse models. It has been used with success to eliminate the mutant allele and delay the progression of cardiomyopathy in *Myh6*-targeted knock-in mice (Jiang J et al, 2013). Knockdown of the mutant allele in *Dnm2* gene restored both muscle force in centronuclear myopathy mouse model and dynamin function in patient-derived fibroblasts (Trochet D et al, 2018). In iPSC-CM carrying the G1681A mutation in *hERG* gene responsible of long-QT syndromes (LQT2) ASP-RNAi leaded to specifically knockdown of the mutant alleles while leaving the wild-type unaffected, maintaining contractibility and structural integrity in cardiomyocytes (Matsa E et al, 2014).

Similarly, silencing of mutant *RyR2* in a catecholaminergic polymorphic ventricular tachycardia (CPVT) mouse model resulted in prevention of arrhythmias and abnormalities of junctional sarcoplasmic reticulum (Bongianino R et al, 2017). Therefore, several experiments have demonstrated the clinical potential of appropriately designed short interfering RNAs in various diseases including viral infections, cardiovascular diseases, cancer and neurodegenerative disorders. In addition, in such a short time from their discovery, several siRNA-based drugs are undergoing clinical trials. Acuity Pharmaceuticals and siRNA Therapeutics with US Food and Drug Administration (FDA) have filed new drug applications to begin clinical trials with modified siRNA molecules in patients with age-related macular degeneration (Reich SJ et al, 2003). The US FDA also approved the use of the siRNA-based drug patisiran (ONPATTRO) for the treatment of hereditary transthyretin amyloidosis (hATTR) with polyneuropathy (Adams D et al, 2018).

The success of gene therapy has largely been driven by improvements in gene delivery systems. Therefore, different viral and non-viral vector systems are used nowadays for gene delivery. Amongst the successful viral vectors, adenovirus, AAV and retrovirus, are the most commonly used vectors (Nayerossadat N et al, 2012). Non-viral vector systems include physical methods such as gene gun, microinjection, electroporation and sonoporation, which employ physical forces to induce the nucleic acid to cross the cell membrane without any carrier agent. Instead, chemical methods including calcium phosphate coprecipitation, cationic liposomes and cationic polymers use chemical agents to transfer the nucleic acid to the cell (Hirai H et al, 1997). Compared with viral methods, non-viral methods may provide several advantages with regard to safety profile, no transgene mis-insertion, DNA/RNA no size limitation and vector mobility. On the contrary, viral gene therapy has shown the have the advantage to exhibit high transduction efficiency in a wide range of human cells, in vivo disease models and clinical trials (Kim TK and Eberwine JH, 2010).

1.5.1 Allele specific silencing by RNA interference (ASP-RNAi)

RNA interference is an evolutionary conserved post-transcriptional gene silencing mechanism that involves double stranded RNA-mediated degradation of target mRNA (Fire A et al, 1998). In the context of autosomal dominant disease, ASP-RNAi, an advanced technique of RNAi, represents a powerful and promising strategy to target mutant alleles leading to its degradation with minimal suppression of the corresponding wild-type allele (Hohjoh H, 2013).

The sequence specific silencing of target mRNA can be triggered by duplex small interference RNA (siRNA), short hairpin RNA (shRNA), miRNA as well as other non-coding RNA (ncRNAs). siRNAs duplex, of 19 nucleotides in size and two nucleotide overhangs at the 3' termini, are generated following a cleavage of long double-strand RNA (dsRNA), >30 nucleotides in size, by the endoribonuclease Dicer (Bernstein E et al, 2001; Costa FF, 2007). The double strands siRNA is incorporated into an RNA-induced silencing complex (RISC) and it is split into passenger and guide strands, the first is then degraded, while the guide strand binds the mRNA target. RISC cleaves the target mRNA, 10 nucleotides from the 5' end of the incorporated siRNA guide strand and the mRNA is degraded by cellular nucleases, resulting in inhibition of target allele expression (Figure 9) (Elbashir SM et al, 2001).

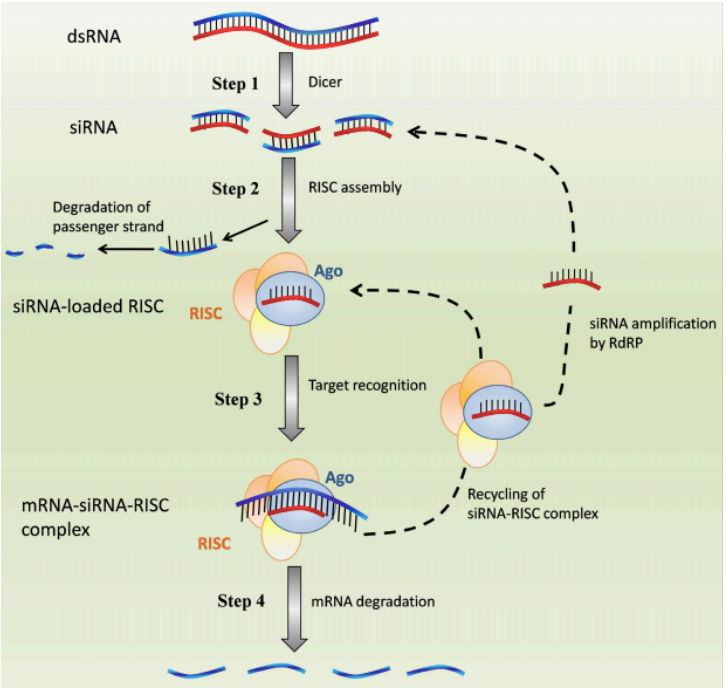

Figure 9. Schematic representation of RNA silencing mechanism in mammalian cell. Long double-stranded RNA (dsRNA) is introduced into the cytoplasm, where it is cleaved into small interfering RNA (siRNA) by the enzyme Dicer. Alternatively, siRNA can be introduced directly into the cell. The siRNA is then incorporated into the RNA-induced silencing complex (RISC), resulting in the cleavage of the sense strand of RNA by argonaute2 (Ago2). The activated RISC-siRNA complex binds to the complementary mRNA, which leads to the silencing of the target gene. The activated RISC-siRNA complex can then be recycled for the destruction of identical mRNA targets (Image from Cuccato G et al, 2011).

The potential of ASP-RNAi appears to be dependent upon its highly sequence-specific knockdown ability; therefore, it is necessary to design siRNAs that confer a strong allele discrimination (Figure 10). An important parameter for designing strong siRNA is the position of nucleotide variation in the siRNA sequence. Different studies demonstrated that siRNAs that carry nucleotide mutation in central positions are able to influence the allele discrimination and perform the correct cleavage activity (Ohnishi Y et al, 2008; Schwarz DS et al, 2006; De Ynigo-Mojado L et al, 2011; Sibley CR et al, 2011).

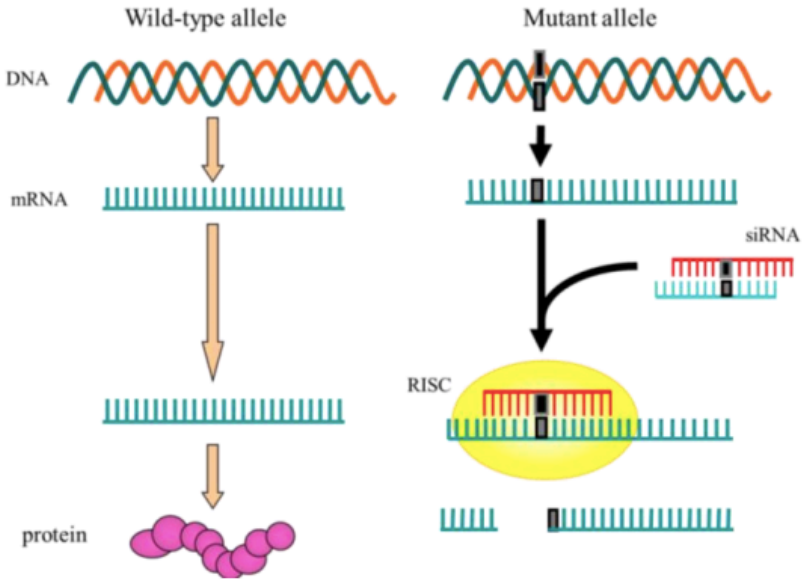

Figure 10. Schematic representation of ASP-RNAi. siRNA duplex carries the nucleotide mutation to specifically discriminate the mutant allele from the wild-type allele (Image from Hohjoh H, 2013).

In addition, since different siRNA duplex targeting the same mutant allele appear to induce different levels of allele specific silencing, several kinds of modifications can be introduced into siRNA sequence to enhance the allele discrimination (Hohjoh H, 2013).

The best effective modification appear to be the introduction of nucleotide mismatches into the siRNAs duplex (Takahashi M et al, 2012; Huang H et al, 2009); however the nucleotide position and the choice of the base are critical aspects to be evaluated. A possible nucleotide position may be the 3'-end of sense siRNA strand (Ohnishi Y et al, 2008). Other possible changes could be the introduction of ribonucleotides chemical modifications, as 2-thiouridine, 5-bromo-uridine, 5-iodio-uridine or 2,6-diaminopurine, which seem to improve the ASP-RNAi (Chiu YL and Rana TM, 2003). In the contrary, the 2'-O-methyl (2'-OMe), 2'-deoxy-2'-fluoro-β-D-arabino-nucleic acids (2'-FANA) and locked nucleic acid (LNA) chemical modifications result in enhancement of longevity of the RNAi activity (Elmen J et al, 2005; Dowler T et al, 2006).

2. Material and Methods

2.1 Cloning of *TNNT2* wild type and mutant sequences in pGL3-TK and pRL-TK plasmids

2.1.1 Preparation of allelic oligonucleotide sequences

Sense and antisense strand of wild-type and mutant oligonucleotide sequences were designed such that nucleotide variation was located at the central position of the sequences and chemically synthesized (Sigma Aldrich) (Table 2 and Table 3). The oligonucleotide sequences include the SphI restriction site for the selection of positive clones; at the 5' and 3' ends of the oligonucleotide sequence cohesive ends matched to the XbaI and NotI digested restriction sites were included for further cloning steps.

Complementary single strands oligonucleotides were annealed in annealing buffer composed by 100 mM Tris-HCl (pH 8), 10 mM EDTA, 1 M NaCl to the final concentration of 100 μM (Hohjoh H. 2010).

Name	Sequences 5'-3'
WT oligo -ss	CTAGCATGCGGACTTTGATGACATCCACC**G**GAAGCGCATGGAGAAGGA
-as	GGCCTCCTTCTCCATGCGCTTC**C**GGTGGATGTCATCAAAGTCCGCATG
R92Q oligo -ss	CTAGCATGCGGACTTTGATGACATCCACC**A**GAAGCGCATGGAGAAGGA
-as	GGCCTCCTTCTCCATGCGCTTC**T**GGTGGATGTCATCAAAGTCCGCATG

Table 2. Sense and antisense strands of wild-type and R92Q oligonucleotide sequences. Mutant nucleotide is shown in bold and SphI restriction enzyme site is underlined.

Name	Sequences 5'-3'
WT oligo -ss	CTAGCATGCGGAAGGCTGAGGATGAGGCC**C**GGAAGAAGAAGGCTTTGT
-as	GGCCACAAAGCCTTCTTCTTCC**G**GGCCTCATCCTCAGCCTTCCGCATG
R173W oligo -ss	CTAGCATGCGGAAGGCTGAGGATGAGGCC**T**GGAAGAAGAAGGCTTTGT
-as	GGCCACAAAGCCTTCTTCTTCC**A**GGCCTCATCCTCAGCCTTCCGCATG

Table 3. Sense and antisense strands of wild-type and R173W oligonucleotide sequences. Mutant nucleotide is shown in bold and SphI restriction enzyme site is underlined.

2.1.2 Construction of reporter expression plasmids

In order to construct reporter expression plasmids, we used the phRL-TK (Promega) and pGL3-TK plasmids (kindly provided by Prof. Hohjoh H, Tokyo, Japan) (Ohnishi Y et al; 2006), which encode the *Renilla reniformis* and *Photinus pyralis* luciferase proteins, respectively. Luciferase genes were driven by the herpes simplex virus thymidine kinase (TK) promoter and they present the restriction sites of XbaI and NotI in their 3'- untranslated regions (UTR). The 48 bp synthetic oligonucleotide duplexes corresponding to the mutants and wild-type *TNNT2* alleles were cloned in the 3'-UTR regions of the luciferase genes. The mutant *TNNT2* sequences were cloned into phRL-TK plasmid and wild type *TNNT2* sequence was cloned into the pGL3-TK plasmid.

Restriction enzyme digestion reactions were performed in a final volume of 150 µl containing 7 µg of reporter plasmids, 15 µl of Buffer D 10X (Promega, Madison, WI, U.S.A), 5 µl BSA 100X (Promega, Madison, WI, U.S.A), 5 µl of XbaI and NotI (10 U/µl) (Promega, Madison, WI, U.S.A). The digestion reactions were incubated at 37°C for 1 hour and the digested reporter plasmids were loaded on 0.8% agarose gel for electrophoresis run in TAE (Tris-acetate-EDTA 40 mM Tris, 20 mM acetic acid, 1 mM EDTA, pH 8.3). 1 µl of SYBR Safe DNA Gel Stain (Invitrogen, Carlsbad, California, USA) per 10 ml of agarose gel was added to detect the band at the end of the run. Before loading the sample in the gel, 1 µl of loading Buffer 6X (0.25% Bromophenol blue;

0.25% Xylene cyanol; 30% glycerol) was added to the DNA samples. At the end of the run, DNA was visualized using an UV transilluminator (220-310 nm) (BioRad, GelDOC1000), the image was captured by a filter Polaroid BX-600 and thermal paper for Polaroid BX-600. The DNA fragments were purified by EuroGOLD Gel Extraction kit (EuroClone) and loaded on 1.5% agarose gel to evaluate DNA concentration using the λ DNA/HindIII Marker 2 (Fermentas). The ligation reaction was optimized to 100 ng of reporter plasmids and for the concentration of oligonucleotide duplexes, using the following formula:

ng of insert = [(ng of plasmid x kb size of insert)/ (kb size of plasmid)]x 3

The ligation reactions were prepared in a final volume of 20 µl composed by 100 ng of either pGL3-TK or pRL-TK plasmid, 3.75 ng of the annealed oligonucleotide duplexes, 2 µl Ligase Buffer 10X (Promega) and 1 µl of T4 DNA Ligase (3 U/µl, Promega) and the ligase reactions were incubated overnight at 16°C.

The following day, the DNA ligation products were dialyzed using MF – Membrane Filters (0.025 µm –Millipore) in order to use it for bacterial cell transformation. The bacterial cell transformation was performed by electroporation at a voltage of 12.5 kV/cm for 4.5-5 msec (MicroPulserElecrtroporator, BioRad); the dialyzed DNA were added to 40 µl of *Escherichia coli X10 GOLD* competent cells and transferred into an electroporation cuvette (MicroPulser Cuvette, 0.1 cm gap, BioRad). Subsequently, bacteria were harvested with 1 ml of SOC-medium (0.5% Yeast Extract, 2% Tryptone, 10 mM NaCl, 2.5 mM KCl, 10 mM $MgCl_2$, 10 mM $MgSO_4$, 20 mM Glucose) in a 15 ml tube and incubated at 37°C for 1 hour under a constant shaking. For selection, bacteria were plated on LB-agar (1% Tryptone, 5% Yeast Extract, 1% NaCl, 1.5% Agar) plates containing 50 µg/ml of ampicillin and incubated overnight at 37°C.

The day after, single colonies were selected from LB-agar plates, transferred to 5 ml LB broth with ampicillin (50 µg/ml) and the bacterial culture was incubated overnight at 37°C at 150 rpm. Plasmid DNA was extracted using the PureLink Quick Plasmid Miniprep Kit (Invitrogen) according to manufacturer's protocol

and the DNA was resuspended in 75 µl of de-ionized H_2O. To check for the presence of the inserted sequences, plasmid DNA was digested in a total volume of 20 µl containing 2 µl of Buffer H 10X (Promega), 0.2 µl of BSA 100X, 100 ng of plasmid DNA, 0,3 µl of SphI restriction enzyme (10 U/µl) (Promega), 2 U of EcoRI restriction enzyme (10 U/µl) (Promega). The reaction mixes were incubated at 37°C for 1 hour and subsequently 10 µl of each reaction was run in 1% agarose gel to visualize the digestion fragments.

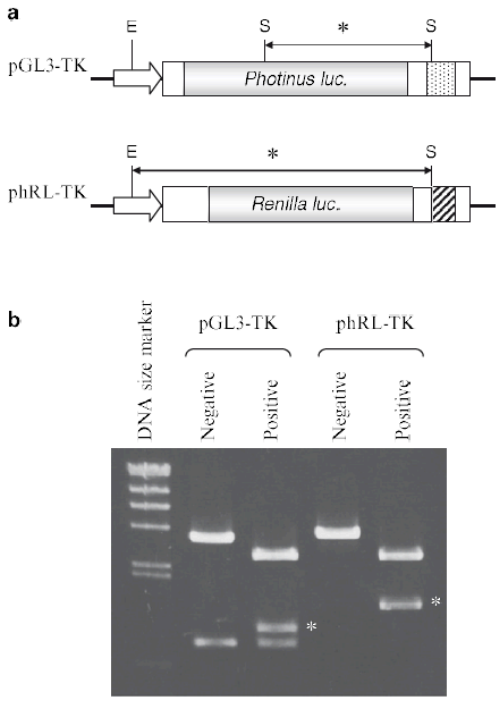

Figure 11. Positive clone selection. (a) Schematic representation of reporter alleles with the SphI (S) and EcoRI (E) restriction enzymes sites. The predicted DNA fragments of positive clones are indicated by asterisks. **(b)** Agarose gel electrophoresis profiles of digested reporter plasmids with SphI and EcoRI. Positive and negative clone examples in each of the reporter plasmids are shown and asterisks indicate the positive fragments obtained as in (a). DNA size marker is λ DNA/HINDIII Marker 2 (Image from Hohjoh H, 2010)

To obtain a large quantity of reporter plasmids the positive bacterial cultures were transferred to 100 ml LB broth supplemented with ampicillin (50 µg/ml).

Plasmid DNA was isolated by PureLink HiPure Plasmid Maxiprep Kit (Invitrogen).

As control, each reporter expression plasmid was sequenced at the Policlinico Santa Maria alle Scotte in Siena with the following sequence primers: primer for pGL3-TK backbone plasmid: 5'- TGTGGACGAAGTACCGAAAG-3'; primer for phRL-TK backbone plasmid: 5'-CTAACACCGAGTTCGTGAAG-3'.

2.2 *TNNT2* full-length sequence amplification

2.2.1 Extraction of RNA and cDNA synthesis

RNA extraction was performed from human cardiac muscle biopsy of healthy donor (kindly donated by Dr. Coppini R, University of Florence) using the miRNeasy Mini Kit (Qiagen, Hilden, Germany). The muscle was weighted and added to 700 µl of Qiazol/100 mg of muscle weight. The cardiac muscle was homogenized with the Tissue Ruptor (Qiagen), by three strokes of five seconds each, rigorously in ice to avoid sample overheating. The lysate was leaved for 5 minutes at room temperature. 140 µl of chloroform were added, the cap tube closed and the sample was shaken vigorously for 15 seconds. After 2-3 minutes at resting condition at room temperature, the sample was centrifuged for 15 minutes at 4°C at 12000 g. Following centrifugation, the homogenate stratified in two phases: the aqueous one, on the upper side, which contains the RNA partition, and the organic one, in the lower side, which contains DNA, proteins and other debris materials. Avoiding the mixing of the phases, the aqueous phase was transferred carefully in a new 1.5 ml tube. 350 µl of 70% ethanol were added and the sample was vortexed. 700 µl of sample were transferred in a RNeasy Mini Spin Column to be centrifuged for 15 seconds at room temperature. The step was repeated. The flow-through was discarded and 700 µl of RWT Buffer were added to the column and then centrifuged at room temperature for 15 seconds at 12000 g. The flow-through was discarded, 500 µl of RPE Buffer were added and the column was centrifuged at room temperature for 15 seconds at 12000 g. The washing step with RPE Buffer was repeated. The column was

centrifuged at the highest speed for 1 minute to eliminate the RPE buffer residuals. The RNeasy Mini Spin Column was placed in a new 1.5 ml tube, 40 µl of RNase-free water were added directly onto the filter present into the column. At the end, to elute RNA, the column was centrifuged at room temperature, at 12000 g for 30 minutes.

The extracted RNA samples were loaded on a 1.2% agarose gel for a horizontal electrophoresis run to verify RNA integrity. 2 µl of RNA sample were diluted with 8 µl of RNase free water and 2 µl 6X DNA Loading Dye (Thermo Fisher Scientific, Waltham, Massachusetts, USA). The electrophoresis run was performed at 70 V for about 45 minutes. The size of RNAs were evaluated using the ladder Gene Ruler 1kb ladder (Thermo Scientific).

2 µg of RNA sample were retrotranscribed in the presence of 0.5 µg of Oligo dT primers/µg RNA in a final volume of 15 µl. The reaction was incubated at 70°C for 5 minutes before adding M-MLV Buffer 5X (Promega), dNTPs 10 mM, RNasin 40 U/µl (Promega), M-MLV Retro-transcriptase 200 U/µl (Promega) and RNAse-free water to a final volume of 25 µl (Table 4). The reaction was incubated for 1 hour at 42°C.

Reagents	**Quantity**	
2 µg RNA	8 µl	STEP 1 5 minutes 70°C
0,5 µg Oligo dT Primers/µg RNA	2 µl	
H_2O	7 µl	
M-MLV Buffer 5X	5 µl	STEP 2 1 hour 42°C
dNTPs 10 mM	2.5 µl	
RNAsin 40 U/µl	1 µl	
M-MLV RT 200 U/µl	1 µl	
H_2O	0.5 µl	

Table 4: Composition of the mix for RNA retrotranscription

The cDNAs were used to perform a control Polymerase Chain Reaction (PCR) with primers for amplification of the housekeeping gene β-actin. 2 µl of cDNA

were amplified in a final volume of 25 µl, using 2.5 µl of Buffer 10X, 2.5 µl of dNTPs (stock 2 mM), 2.5 µl of forward and reverse primers for β-actin (stock 10 µM), 0.25 µl of Dream-Taq (stock 5 U/µl) (Thermo Scientific). The temperatures, cycle time, and the number of cycles of the program of amplification are reported in the Table 5.

Temperature (°C)	Time	Cycle
95	5 min	1x
95	30 sec	30x
54	30 sec	
72	45 sec	
72	10 min	1x
4	HOLD	

Table 5. Amplification program for β-actin.

The amplified product of the PCR reaction was resolved by horizontal electrophoresis run with a 2% agarose gel, for 30 minutes at constant voltage of 130 V. The length in term of base pair (bp) of amplification product was evaluated using the Gene Ruler 100 bp ladder (Thermo Fisher Scientific).

2.2.2 Amplification of wild type *TNNT2* sequence

The *TNNT2* cDNA was amplified with a master mix containing 2.5 µl of Dream Buffer 10X, 2.5 µl of dNTPs (stock 2 mM), 2.5 µl of forward and reverse primers (stock 10 µM) (Table 7), 0.25 µl of Dream-Taq DNA polymerase (stock 5 U/µl), 5 µl of cDNA and water to reach the final volume of 25 µl. Cycle times, the temperatures and the number of cycles of the amplification program are reported in the Table 6.

Temperature (°C)	Time	Cycles
95 °C	5 min	1x
94 °C	1 sec	25 x
56 °C	1 sec	
72 °C	1 sec	
72 °C	10 min	1x
4 °C	HOLD	

Table 6. *TNNT2* gene amplification program

Gene	Forward primer sequence (5'-3')	Reverse primer sequence (5'-3')	Tm (°C)
TNNT2	CCCGCTGAGACTGAGCAGA	AGGCCAGCTCCCCATTTCC	56

Table 7. Primers sequences for *TNNT2* gene synthesis

The product of the PCR reaction was resolved by electrophoresis run in a 0.8% agarose gel. The electrophoresis run was performed in horizontal electrophoresis cell (Bio-Rad, Hercules, California, USA), for about 30 minutes at constant voltage of 130V, using an Electrophoresis Power Supply (EPS 600, Amersham Pharmacia Biotech, Little Chalfont, UK). The length in term of base pair (bp) of the amplification product was evaluated using a Gene Ruler 100 bp ladder with bands with known lengths. DNA fragment corresponding to *TNNT2* was excised using an UV light box. The purification was performed by EuroGOLD Gel Extraction kit. The purified DNA was visualized in 1.5% agarose gel using λ DNA/HindIII Marker 2.

2.3 Cloning of *TNNT2* wild-type sequence in eukaryotic expression plasmid

2.3.1 Construction of pGEM-T-Easy- *TNNT2* wild type plasmid

The *TNNT2* wild type full-length sequence was sub-cloned into the pGEM-T-Easy vector (Promega). pGEM-T-Easy vector (Figure 12) is a linearized vector with a single 3'-terminal thymidine at both ends to greatly improve the efficiency of ligation of PCR products by preventing recircularization of the vector.
The ligation reaction was optimized to 50 ng of pGEM T-Easy vector and for the concentration of TNNT2, using the following formula:

ng of insert = [(ng of vector x kb size of insert)/ (kb size of vector)]x 3

The ligation reaction was performed in a final volume of 20 µl using 2 µl of Ligase Buffer 10X, 1 µl of T4 DNA Ligase (3 U/µl), 50 ng of pGEM-T-Easy and 50 ng of TNNT2 purified cDNA and the ligation reaction was incubated at 16°C overnight. The day after, the DNA ligation product was dialyzed using MF – Membrane Filters (0.025 µm) in order to use it for bacterial cell transformation. Positive colonies were selected by colony PCR using T7 and SP6 primers (stock 10 µM) (Table 8).

Primer	Sequences 5'-3'
SP6	ATTTAGGTGACACTATAG
T7	TAATACGACTCACTATAGGG

Table 8. SP6 and T7 primer sequences

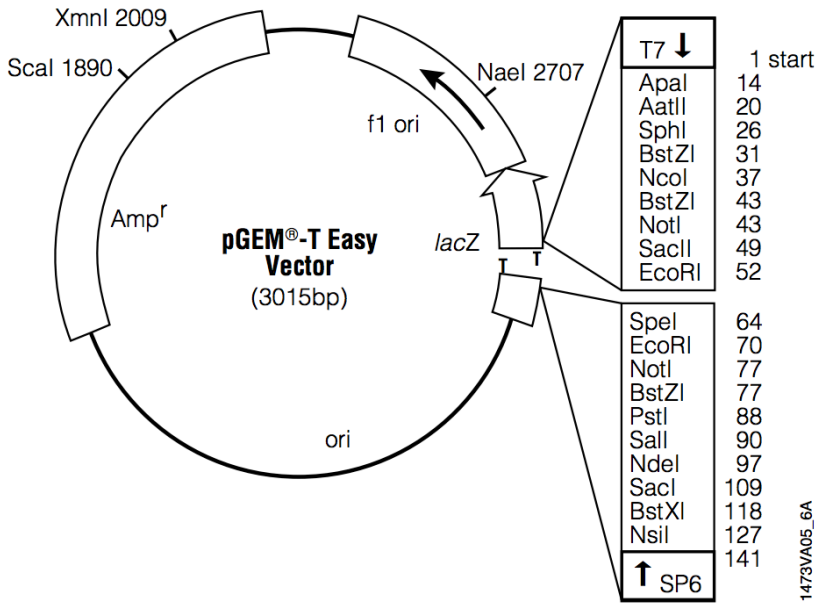

Figure 12. pGEM®-T Easy Vector map and sequence reference points

The temperatures, cycles time, and the number of cycles of the program of amplification reaction are reported in the Table 9.

Temperature (°C)	Time	Cycle
95	5 min	1x
95	1 sec	25 x
56	1 sec	
72	1 sec	
72	10 min	1x
4	HOLD	

Table 9. Colony PCR program for pGEM-T-Easy-*TNNT2*

Positive colonies were diluted in 5 ml LB broth with ampicillin (50 µg/ml) and incubated overnight at 37°C at 150 rpm. The DNA plasmid isolation was performed by the PureLink Quick Plasmid Miniprep Kit. Plasmid DNA was digested to confirm the presence of the TNNT2 cDNA. To obtain a large quantity of pGEM-T-Easy-*TNNT2*, the positive bacterial culture was diluted to 100 ml

LB broth supplemented with ampicillin (50 µg/ml). Plasmid DNA was isolated by PureLink HiPure Plasmid Maxiprep Kit.

As control, each plasmid was sequenced at the Policlinico Santa Maria alle Scotte in Siena.

2.3.2 Construction of pcDNA3-*TNNT2* wild type expression plasmid

In order to generate the pcDNA3-*TNNT2* expression plasmid, the TNNT2 sequence was isolated from the pGEM-T-Easy-*TNNT2* vector and subcloned into the pcDNA3 vector using the EcoRI restriction site (Figure 13). Plasmids were digested in a final volume of 150 µl as follow: 15 µl of Buffer H 10X, 1.5 µl of BSA 100X, 10 µg of pcDNA3 or pGEM-T-Easy-*TNNT2*, 1.5 µl of EcoRI (10 U/µl). The reaction mixes were incubated at 37°C for 2.5 hours; 1 µl of Thermosensitive Alkaline Phosphatase (TSAP) (Promega) was added to the pcDNA3 digestion reaction and incubated at 37°C 15 minutes to dephosphorylate the ends and prevent re-circularization. TSAP activity was inactivated at 74°C for 17 minutes.

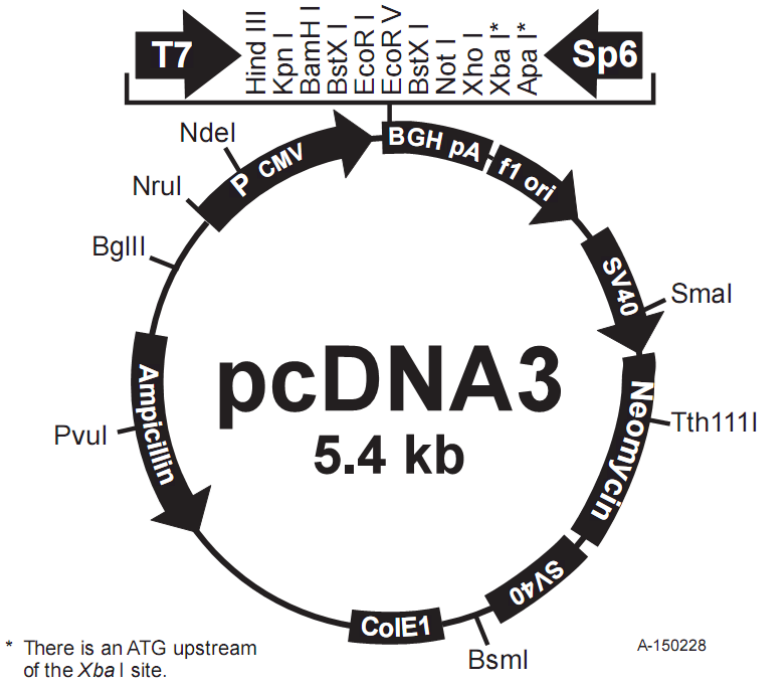

Figure 13. pcDNA3 vector map and sequence reference points.

The DNA fragments obtained were loaded on 0.8% agarose gel for electrophoresis run to purify the DNA fragments of 1040 and 5400 bp, corresponding to *TNNT2* and linear pcDNA3 respectively. The DNA fragments were purified by EuroGOLD Gel Extraction kit and then loaded on 1.5% agarose gel for electrophoresis run to evaluate DNA concentration using the λ DNA/HindIII Marker 2.

The ligation reaction was optimized for 100 ng of pcDNA3 plasmid using the following formula:

ng of insert = [(ng of vector x kb size of insert)/ (kb size of vector)] x 3

The ligation reaction was performed in a final volume of 20 µl using 2 µl of Ligase Buffer 10X, 1 µl of T4 DNA Ligase (3 U/µl), 100 ng of pcDNA3, 80 ng of *TNNT2* DNA and the ligation reaction was incubated at 16°C overnight. The day after, the DNA ligation product was dialyzed using MF-Membrane Filters (0.025 µm) in order to use it for bacterial cell transformation.

Positive colonies were selected by colony PCR using primers specific for the TNNT2 sequence.

The temperatures, cycles time, and the number of cycles of the program of amplification reaction are reported in the Table 10.

Temperature (°C)	Time	Cycle
95	5 min	1x
95	1 sec	25 x
56	1 sec	
72	1 sec	
72	10 min	1x
4	HOLD	

Table 10. Colony PCR program for pcDNA3-*TNNT2*

Positive colonies were diluted to 5 ml LB broth with ampicillin (50 µg/ml) and incubated overnight for plasmid purification. Plasmid DNA was isolated by the use of PureLink Quick Plasmid Miniprep Kit and subsequently digested to confirm the cloning of the *TNNT2* sequence-.

To obtain a large quantity of pGEM-T-Easy-*TNNT2*, the positive bacterial culture was diluted to 100 ml LB broth supplemented with ampicillin (50 µg/ml). Plasmid DNA was isolated by PureLink HiPure Plasmid Maxiprep Kit.

As control, each reporter expression plasmid was sequenced at the Policlinico Santa Maria alle Scotte in Siena.

2.4 Cloning of *TNNT2*-R92Q and *TNNT2*-R173W sequences in eukaryotic expression plasmid

2.4.1 Site-directed mutagenesis

Site-directed mutagenesis was performed by PCR and the pcDNA3-*TNNT2* as DNA template. Site-directed mutagenesis by primer extension was performed by incorporating DNA oligonucleotides containing the desired mutation in independent, nested PCRs before combining them in the final product (Table 12). The reaction requires flanking primers (a and d; Figure 14) complementary to the ends of the *TNNT2* sequence, and two internal complementary primers (b and c; Figure 14). containing either the c.275 G>A or c.517 C>T corresponding to the R92Q or R173W mutations, respectively.

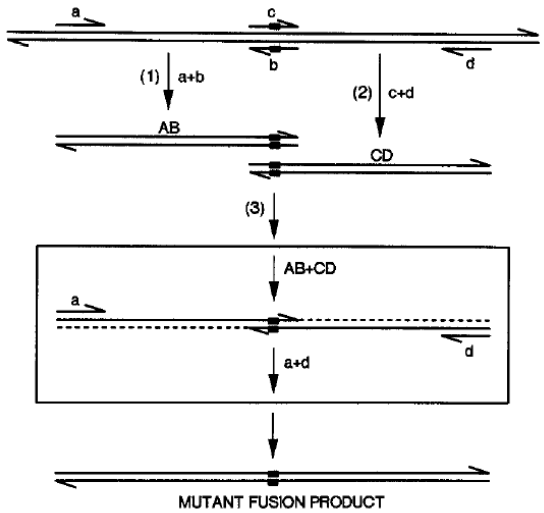

Figure 14. Schematic representation of site-directed mutagenesis by overlap extension. Double strands DNA and primers are shown by lines with 5'-3' orientation. The site of mutagenesis is indicated by small black spot. The final mutant product is obtained by amplified of the two fragments carrying the mutation (Image from Ho SN et al, 1989).

During the first round of PCR, AB and CD fragments are created (Figure 14). To amplify the AB fragment the forward primer for mutant TNNT2 (for R92Q or R173W mutation) and SP6 primer were used, whereas to amplify the CD fragment the T7 primer and reverse primer for mutant TNNT2 (Table 13) were used. The two PCR reactions were performed in a final volume of 25 µl, as follows: 100 ng of DNA template, 2.5 µl PfU Buffer 10X (Promega), 2.5 µl of dNTPs (from a stock solution 2 mM), 0.5 µl of PfU DNA polymerase (3 U/µl, Promega), 1 µl of each couple of primers (10 µM).

The temperatures, cycle times, and the number of cycles of the amplification program are reported in the Table 11.

Temperature	Time	Cycle
95	5 min	1x
95	1 sec	30 x
56	1 sec	
72	1 sec	
72	10 min	1x
4	HOLD	

Table 11. Amplification program for AB and CD generation fragments

The fragments obtained were loaded on 0.8% agarose gel for electrophoresis run to purify the DNA fragments of 560 and 840 bp or 697 and 721 bp corresponding to R92Q and R173W mutation, respectively. The DNA fragments were purified by EuroGOLD Gel Extraction kit and then loaded on 0.8% agarose gel for electrophoresis run to evaluate DNA concentration using a λ DNA/HindIII Marker 2.

The purified products were ligated by a second PCR using flanking primers (Table 7).

The second PCR reaction mixes were performed in a final volume of 100 µl using 100 ng of AB purified product, 100 ng of CD purified product, 10 µl PfU Buffer 10X (Promega), 10µl of dNTPs (from a stock solution of 2 mM), 1µl of PfU DNA polymerase (3 U/µl, Promega). The reactions were incubated as in table 12A. At the end of the incubation 10 µl of the flanking primers (10 µM) were added to the reaction mix to amplify the mutant fusion product (Table 12B). The temperatures, cycle times, and the number of cycles of the amplification program are reported in the Table 12.

A

Temperature (°C)	Time	Cycles
95 °C	5 min	1x
52 °C	15 min	
72 °C	10 min	

B

Temperature (°C)	Time	Cycles
95 °C	5 min	1x
95 °C	1 min	25x
52°C	1 min	
72°C	2,30 min	
72°C	10 min	1x

Table 12. (A-B) Amplification program for *TNNT2* mutant sequences

	Forward primer sequence (5'-3')	Reverse primer sequence (5'-3')
R173W	GAGGATGAGGCCTGGAAGAAGAAGG	CCTTCTTCTTCCAGGCCTCATCCTC
R92Q	ATGACATCCACCAGAAGCGCATGGA	TCCATGCGCTTCTGGTGGATGTCAT

Table 13. Site-directed mutagenesis primers

2.4.2 Construction of pcDNA3-*TNNT2*-R92Q and pcDNA3-*TNNT2*-R173W expression plasmid

The *TNNT2*-R92Q and *TNNT2*-R173W mutant fusion products were sequenced and cloned in pcDNA3 expression plasmid, as described in 2.3.2.

2.5 Cell line

293T human embryonic kidney (HEK293T) cells were grown in Dulbecco's modified Eagle's medium (DMEM) (Sigma Aldrich) supplemented with 10% heat inactivated fetal bovine serum (Sigma Aldrich), 100 U/ml penicillin, 100 μg/ml streptomycin, 2 mM L-glutamine, 1 mM sodium pyruvate at 37°C in a 5% CO_2 humidified atmosphere.

2.6 Design of siRNAs

Lyophilized silencing RNA oligonucleotides (siRNAs) were purchased from Sigma Aldrich (St. Louis, Missouri, U.S.A.) and resuspended in the provided buffer at a final concentration of 20 μM (Tables 14-17). In each experiment, they were used at a final concentration of 200 nM. Non-silencing siRNA duplexes (AM4605, Ambion) were used as a negative control.

Name		Sequences 5'-3'
siRNA A10	-ss	ACAUCCACC**A**GAAGCGCAUGGUU
	-as	CCAUGCGCUUC**U**GGUGGAUGUUU
siRNA A11	-ss	GACAUCCACC**A**GAAGCGCAUUU
	-as	AUGCGCU**U**CUGGUGGAUGUCUU
siRNA A12	-ss	UGACAUCCACC**A**GAAGCGCAUUU
	-as	AUGCGCUUC**U**GGUGGAUGUCAUU
siRNA A10	-ss	ACAUCCACC**A**GAAGCGCAUUU
	-as	AUGCGCUUC**U**GGUGGAUGUUU

Table 14. Synthetic 21-mer siRNAs and 19-mer siRNA duplex targeting R92Q mutation with 3'-dTdT overhangs. The mutant base is shown in bold letter.

Name		Sequences 5'-3'
siRNA10 (U13)	-ss	ACAUCCACC**A**GA**U**GCGCAUUU
	-as	AUGCGC**A**UC**U**GGUGGAUGUUU
siRNA A10(C14)	-ss	ACAUCCACC**A**GAA**C**CGCAUUU
	-as	AUGCG**G**UUC**U**GGUGGAUGUUU
siRNA A10(U15)	-ss	ACAUCCACC**A**GAAG**U**GCAUUU
	-as	AUGC**A**CUUC**U**GGUGGAUGUUU

Table 15. Synthetic 19-mer siRNAs duplex targeting R92Q with 3'-dTdT overhangs. The base variations are shown in bold letter and the supplemental mismatch is shown in bold and underlined.

Name		Sequences 5'-3'
siRNA U9	-ss	AUGAGGCC**U**GGAAGAAGAAUU
	-as	UUCUUCUUCC**A**GGCCUCAUUU
siRNA U10	-ss	GAUGAGGCC**U**GGAAGAAGAAUU
	-as	UUCUUCUUCC**A**GGCCUCACUUU
siRNA U11	-ss	GGAUGAGGCC**U**GGAAGAAGAAUU
	-as	UUCUUCUUCC**A**GGCCUCACCUUU
siRNA U12	-ss	AGGAUGAGGCC**U**GGAAGAAGAAUU
	-as	UUCUUCUUCC**A**GGCCUCAUCCUUU

Table 16. Synthetic 19-mer siRNAs duplex targeting R173W with 3'-dTdT overhangs. The base variation is shown in bold letter.

Name		Sequences 5'-3'
siRNA U9(U13)	-ss	AUGAGGCC**U**GGA**U**GAAGAAUU
	-as	UUCUUC**A**UCC**A**GGCCUCAUUU
siRNA U9(C14)	-ss	AUGAGGCC**U**GGAA**C**AAGAAUU
	-as	UUCUU**G**UUCC**A**GGCCUCAUUU
siRNA U9(U15)	-ss	AUGAGGCC**U**GGAAG**U**AGAAUU
	-as	UUCU**A**CUUCC**A**GGCCUCAUUU
siRNA U12(C14)	-ss	AGGAUGAGGCC**U**G**C**AAGAAGAAUU
	-as	UUCUUCUU**G**C**A**GGCCUCAUCCUUU
siRNA U12(U15)	-ss	AGGAUGAGGCC**U**GG**U**AGAAGAAUU
	-as	UUCUUCU**A**CC**A**GGCCUCAUCCUUU

Table 17. Synthetic 19-mer siRNAs duplex targeting R173W with 3'-dTdT overhangs. The base variations are shown in bold letter and the supplemental mismatch is shown in bold and underlined.

2.7 Transfection and luminescent assays

The day before the transfection HEK293T cells were detached by trypsin-EDTA (0.05% trypsin, 0.53 mmol/L EDTA·4Na) at 70%-90% confluency, resuspended in fresh medium and seeded into 24-well culture plates at the density of 0.5 x 10^5 cells/well to perform luciferase report assay or into 60 mm dishes at the density of 1 x 10^6 cells/dish to perform western blot analysis. Co-transfection with synthetic siRNA duplex and reporter plasmids was carried out using Lipofectamine transfection Reagent (Invitrogen, Carlsbad, USA) and Oligofectamine Reagent (Invitrogen, Carlsbad, USA) according to the manufacturer's instructions. Before co-transfection, the culture medium was replaced with antibiotics free DMEM, and cells in each well were transfected with 0.2 μg of reporter plasmids, 0.1 μg of pSV-β-Galactosidase control vector (Promega) and 200 nM of siRNA duplex. Cells were incubated for 3 h at 37°C and then fresh culture medium with 20% fetal bovine serum was added and cells were then incubated at 37°C for twenty-four hours. Cells were lysed using passive lysis buffer (Promega) and the expression levels of luciferase and β-Galactosidase were analyzed by the Dual-Luciferase report assay system (Promega) and Beta-Glo assay system (Promega). 20 μl of cell lysate were transferred into a luminometer tube containing the Luciferase Assay Reagent II to generate and stabilize the luminescent signal of the *Photinus* luciferase. The *Renilla* luciferase reaction was simultaneously initiated by adding Stop & Glo Reagent to the same tube. 20 μl of cell lysate were used to measure the β-Galactosidase activity by the addition the Beta Glo Reagent into the luminometer tube. The luminescence intensity of both luciferases and β-Galactosidase was determined by a luminometer (TD20/20). Levels of either mutant and wild type luciferases were normalized on the levels of β-Galactosidase activity. The ratio of mutant and wild-type luciferase activities in the presence of siRNAs targets were normalized on the ratio obtained in the presence of control siRNA. Statistical analysis was performed by Student t-test analysis.

2.8 Western blot analysis

Cells were collected 24 hours after transfection, washed twice with ice-cold PBS (Sigma-Aldrich), harvested by centrifugation at 12000 x g for 1 min at 4 °C and lysed in lysis buffer (50 mM Tris-Cl pH 7.4, 150 mM NaCl, 1% NP-40, 1 mM EDTA, 0.25% Sodium deoxicholate) supplemented with 1x protease inhibitors cocktail and 0.1 mM PMSF (phenylmethylsulfonyl fluoride). Cells were collected and incubated for 1h at 4°C and sonicated (30 pulse, 30% power; Bandelin Sonopuls). Protein concentration was measured using Protein Assay Dye Reagent Concentrate kit (Bio-Rad, Munchen, Germany) at Ultraspec 2100 pro UV/Visible Spectrophotometer (Amersham Bioscience). Equal amounts of protein (100 μg) were mixed with 4x sample buffer (250 mM Tris HCl ph 6.8, 8% SDS, 40% Glycerol, 20% beta-mercaptoethanol, 0.016% bromophenol blue) boiled for 5 minutes at 95°C and separated by SDS-PAGE on 10% polyacrylamide gel using TGS 1X running buffer (25 mM Tris, 190 mM glycine and 1% SDS) at 25 mA for 90 minutes at room temperature. After electrophoresis, proteins were blotted into nitrocellulose blotting membrane (GE healthcare, Life science, Germany) using a transfer buffer (25mM Tris, 190 mM glycine, 15% methanol and 0.1 % SDS) at 400 mA for 2 h in a cold room. The membrane was incubated for 1 hour in blocking solution with 5% Bovine Serum Albumin (BSA)(Sigma-Aldrich) in TBS-T (150 mM NaCl, 10 mM Tris, pH 7.4, 0.2% Tween-20) and then incubated with primary antibodies (described below) at 4°C overnight; membranes were washes in TBS-T buffer, and further incubated with 1:3000 diluted horseradish peroxidase-conjugated goat anti-mouse IgG (Amersham) for 1 h at room temperature.

Antigen-antibody complexes were visualized using Immobilon Western Chemiluminescent HRP Substrate (Bio-Rad) and the images were acquired with Chemidoc MP (Bio-Rad) The intensity of the bands was quantified using Image Lab^{TM} Software (Bio-Rad). The primary antibodies used in Western blotting and their dilution were as follows: monoclonal anti-cTnT (1:200) (Invitrogen) and monoclonal anti-GFP (1:1000) (Sigma-Aldrich).

3. Results

3.1 Amplification of TNNT2 by Polymerase Chain Reaction (PCR) and construction of pcDNA3-TNNT2 expression plasmid

To generate the pcDNA3-TNNT2-expression plasmid, the full-length coding sequence of TNNT2 (NM_001001430.3) was previously amplified from cardiac tissue cDNA by Polymerase Chain Reaction (PCR). The amplification of TNNT2 was verified by agarose gel electrophoresis run; the band of 1058 bp, corresponding to TNNT2 sequence is shown in Figure 15.

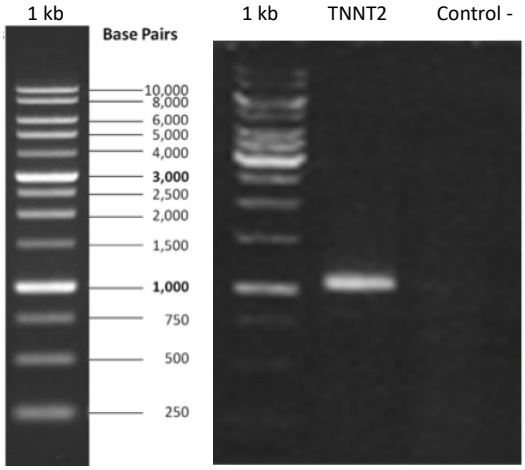

Figure 15. Qualitative PCR of TNNT2 amplification. Lane 1 marker 1kb, lane 2 TNNT2 amplified fragment, lane 3 negative control.

Subsequently, the purified TNNT2 DNA was cloned in pcDNA3 plasmid, designed for high-level expression in mammalian cell lines, as described in paragraph 2.3.2. The resulting 6651 bp pcDNA3-TNNT2-wt expression plasmid is a circular plasmid containing the TNNT2 full-length sequence, the Cytomegalovirus (CMV) enhancer-promoter for high-level expression, the SV40 origin of replication, ampicillin and neomycin resistance (Figure 16).

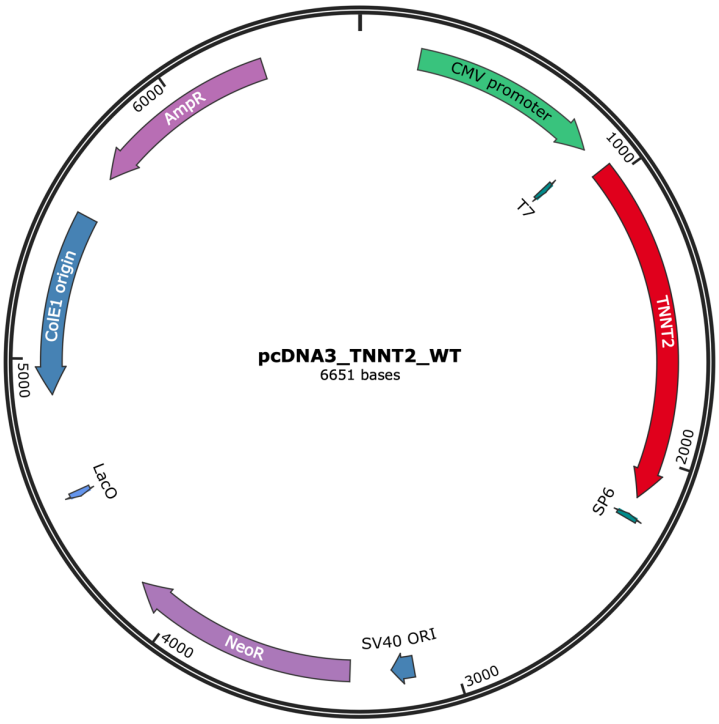

Figure 16. Sequence map of pcDNA3-TNNT2-wt expression plasmid.

3.2 Site-directed mutagenesis and construction of pcDNA3-TNNT2-R92Q and pcDNA3-TNNT2-R173W expression plasmids

To generate mutant expression plasmids, the site directed mutagenesis on TNNT2 sequence was performed by primer extension PCR (see 2.4.1 for details).

Figure 17A shows the 560 bp and 840 bp fragments generated by independent PCR reactions using overlapping mutagenized primers for the R92Q sequence. The purified PCR fragments containing the mutation were used as template for a new PCR reaction to amplify the 1400 bp full-length TNNT2 sequence containing the R92Q mutation (Figure 17B). The same approach was used to generate the TNNT2 sequence carrying the R173W mutation.

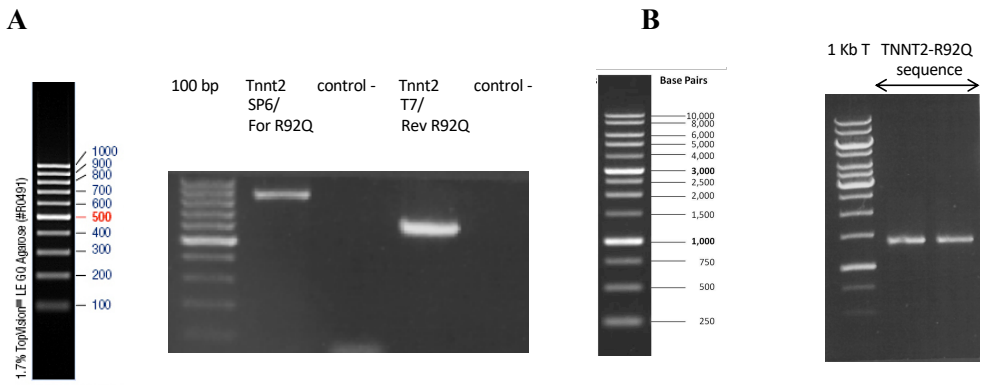

Figure 17. Site directed mutagenesis. (A) Lane 1 marker 100 bp, lane 2 and 4 PCR products of 840 bp and 560 bp carrying the R92Q mutation, lane 3 and 5 negative controls. **(B)** Lane 1 marker 1kb, lane 2 and 3 full-length TNNT2 mutant sequence amplified using purified PCR products as a template in the second PCR.

Finally, the TNNT2-R92Q and TNNT2-R173W sequences were cloned in pcDNA3 plasmid as described in section 2.4.2. The resulting 6651 bp pcDNA3-TNNT2-R92Q and pcDNA3-TNNT2-R173W expression plasmids are circular plasmids containing each one the TNNT2 mutant sequence, Cytomegalovirus (CMV) enhancer-promoter for high-level expression, the SV40 origin of replication, ampicillin and neomycin resistance (Figure 18A, 18B).

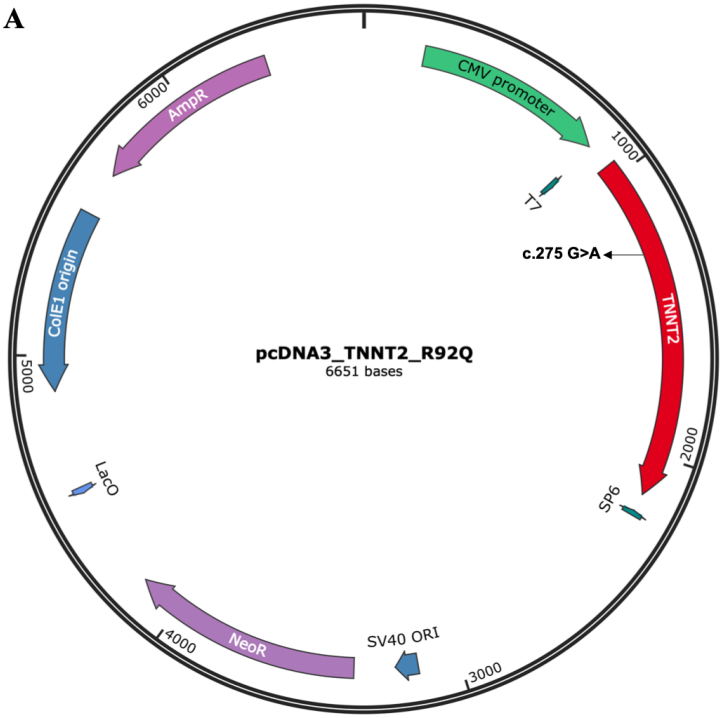

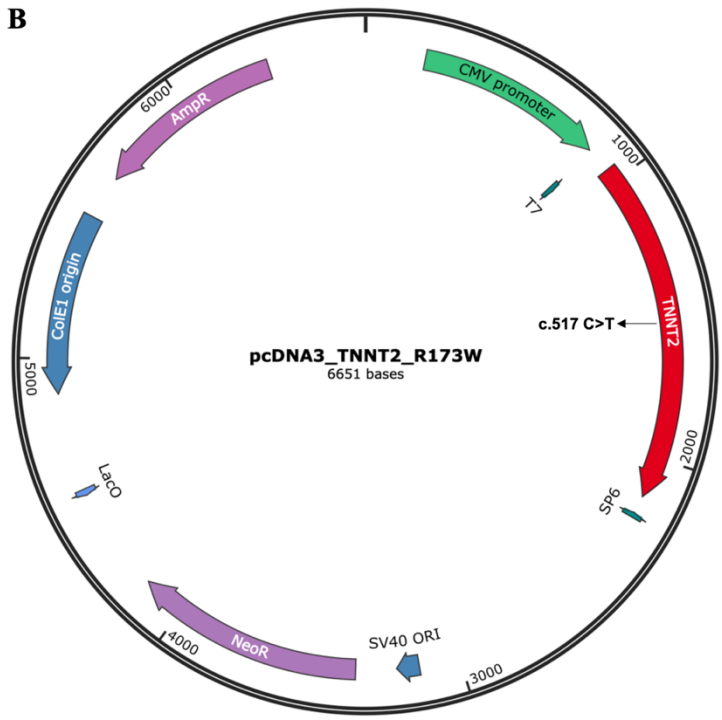

Figure 18. (A) Maps of pcDNA3-TNNT2-R92Q and **(B)** pcDNA3-TNNT2-R173W expression plasmids.

3.3 ASP-RNAi of *TNNT2*-R92Q using 21-mer siRNAs

In order to achieve allele specific silencing of mRNAs containing the TNNT2 R92Q mutation, three 21-mer siRNAs complementary to the sequence of the mutant TNNT2 and carrying the c.275 G>A substitution at positions +10, +11 or +12 of their sequence were designed (Figure 19A). Silencing efficiency and allele discrimination were evaluated by the dual luciferase reporter assay. To this aim, a 37 nucleotides fragment from either human wild type or R92Q mutant TNNT2 sequence were cloned in the 3'-UTR of genes coding for *Photinus pyralis* and *Renilla reniformis* luciferases, respectively (Figure 19B). As shown in figure 20, all siRNAs duplexes analyzed inhibited the expression of both luciferases, with no statistically significant allele-specific silencing. In detail, the residual expression of the mutant TNNT2 allele ranged from 32 ± 8.5% to 20 ± 3.6% and that of the WT TNNT2 allele ranged from 43 ± 13% to 30 ± 6.5%, as compared to control siRNA.

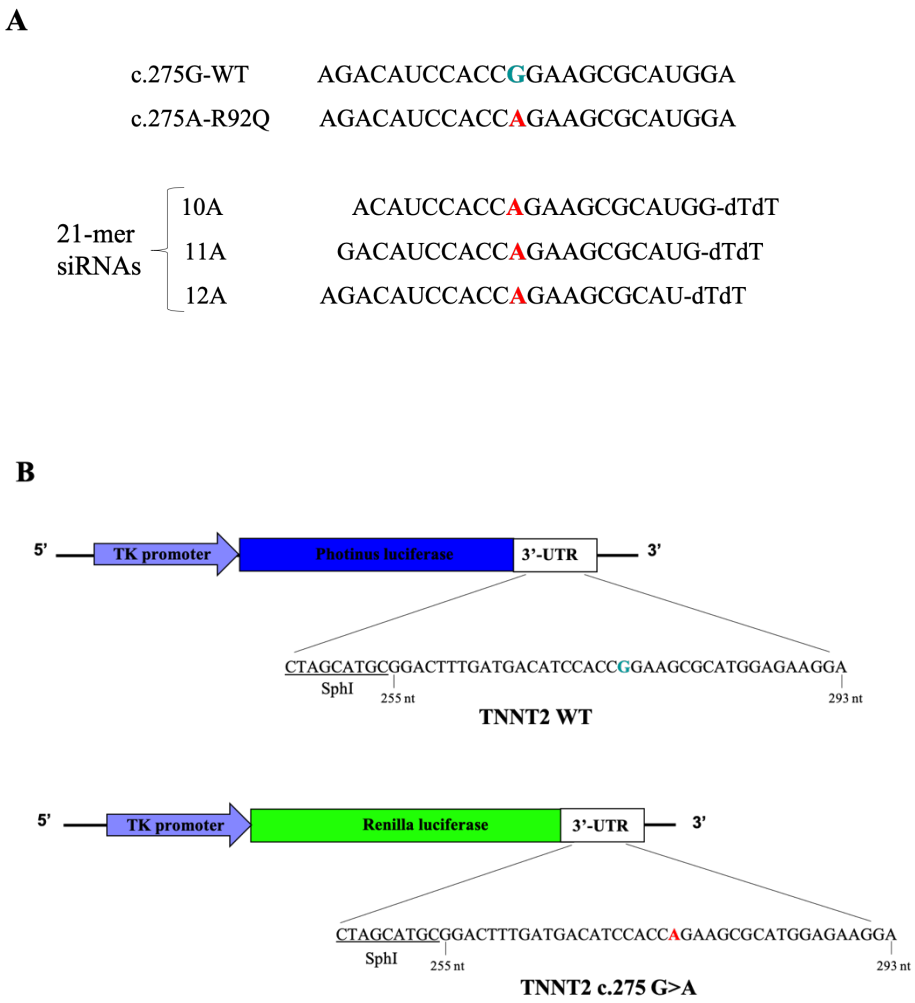

Figure 19. Design of siRNAs sequences and representation of reporter alleles. (A) Sequences of 21-mer sense-strand siRNAs (10A-12A) targeting the R92Q mutation. The nucleotide corresponding to the A mutation is shown in bold and red and the original G nucleotide is in bold and green. **(B)** Schematic maps of reporter alleles. Reporter alleles were constructed based on *Photinus pyralis* and *Renilla reniformis* luciferase genes transcribed starting from the TK promoter and containing in their 3'-UTR the sequences of the wild type or mutant alleles, respectively. Nucleotides from +255 to +293 respect to the start codon refer to the human TNNT2 cDNA sequence (NM_001001430.3).

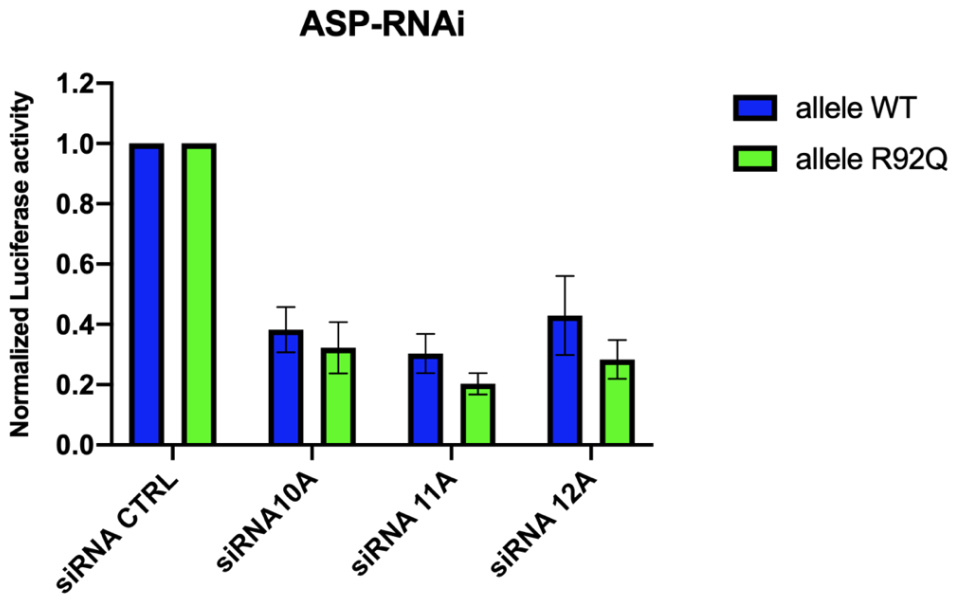

Figure 20. Assessment of ASP-RNAi on reporter alleles. Luciferase activity measured in HEK293T cells transfected with *Renilla* and *Photinus* luciferase expression plasmids. Luciferase levels were normalized against the levels of β-galactosidase activity. The β-galactosidase-normalized luciferase activity measured in the presence of siRNA duplexes were referred to the luciferase activity measured in the presence of control siRNA. Data are presented as mean ± S.D. of four independent experiments.

3.4 ASP-RNAi of *TNNT2*-R92Q using 19-mer siRNAs

In order to improve the allele specificity of RNA interference, a single base mismatch was introduced in the sequence of the siRNA. In particular, based on the analysis of silencing specificity, the sequence of the 12A siRNA was selected to design shorter 19-mer siRNAs containing the G>A substitution at position 10 and containing a single base mismatches in the seed region (A>U G>C and C>U in positions 13, 14 and 15, respectively) (Figure 21A). As control, a 19-mer siRNA containing only the G>A substitution was also tested. siRNAs were tested by luciferase assay and the effects on luciferase activity of the 19-mer siRNAs are show in Figure 21B.

The results obtained showed that 19-mer 12A siRNA induces a more significant silencing of the mutant allele (92.4 ± 4%), compared to the 21-mer 12A siRNA (79.7 ± 3.6%). Analysis of the 19-mer 12A siRNA containing a single base mismatch showed that the 12A(13U) siRNA induced the more efficient allele

discrimination, with a silencing of 83.1 ± 2.7% of the luciferase mRNA carrying the mutant allele and only a 12.8 ± 5.2% inhibition of the WT allele. In contrast, although both 19-mer 12A(14C) and 12A(15U) siRNAs showed a significant allele specificity, they also induced a strong reduction in the expression of the luciferase mRNA corresponding to the WT allele.

A

	c.275G-WT	AGACAUCCACC**G**GAAGCGCAUGGA
	c.275A-R92Q	AGACAUCCACC**A**GAAGCGCAUGGA
19-mer siRNAs	12A	ACAUCCACC**A**GAAGCGCAU-dTdT
	12A(13U)	ACAUCCACC**A**GA**U**GCGCAU-dTdT
	12A(14C)	ACAUCCACC**A**GAA**C**CGCAU-dTdT
	12A(15U)	ACAUCCACC**A**GAAG**U**GCAU-dTdT

B

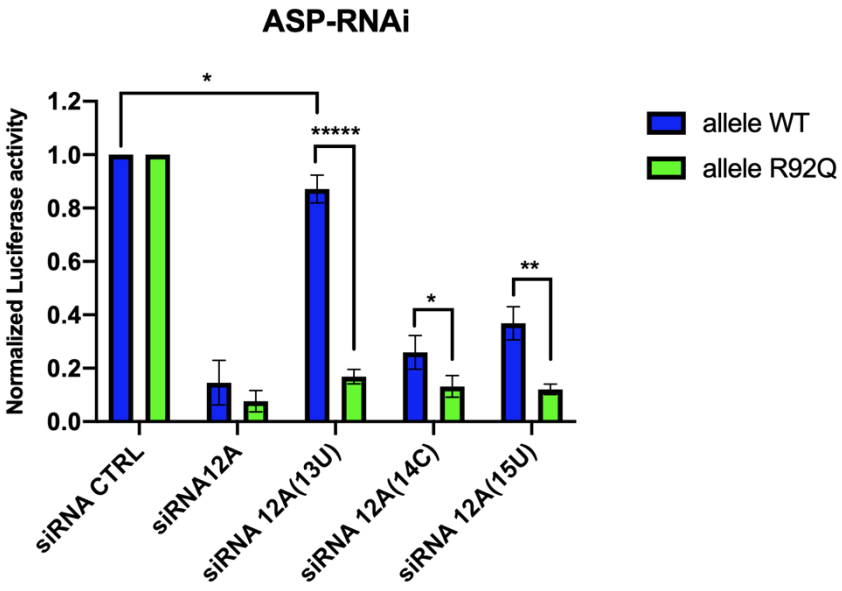

Figure 21. Assessment of ASP-RNAi on reporter alleles. (A) 19-mer sense-strand siRNA 12A and 19-mer sense-strand siRNAs 12A carrying a mismatch targeting the R92Q mutation. The nucleotide corresponding to the A mutation is shown in bold and red, the original G nucleotide is in bold and green and the single base mismatch is shown

in bold, red and underlined. **(B)** Luciferase activity measured in HEK293T cells transfected with *Renilla* and *Photinus* luciferase expression plasmids. Luciferase levels were normalized against the levels of β-galactosidase activity. The β-galactosidase-normalized luciferase activity measured in the presence of siRNA duplexes were referred to the luciferase activity measured in the presence of control siRNA. Data are presented as mean ± S.D. of four independent experiments (*$p<0.05$, **$p<0.005$ and *****$p<0.000005$).

3.5 ASP-RNAi of *TNNT2*- R173W

To induce ASP-RNAi of mutant mRNAs containing the TNNT2 R173W mutation, four 19-mer siRNAs duplex complementary to the sequence of the mutant TNNT2 and carrying the c.517, C>T substitution at position +9, +10, +11 and +12 of their sequence were designed (Figure 22A). Silencing efficiency and allele discrimination were evaluated by the dual luciferase reporter assay. To this aim, a 37 nucleotides fragment from either human wild type or R173W mutant TNNT2 sequence were cloned in the 3'-UTR of genes coding for *Photinus pyralis* and *Renilla reniformis* luciferases, respectively (Figure 22B).

The luciferase assay showed that siRNA 9U, 11U and 12U achieved a significant ASP-RNAi and, specifically, siRNA 9U and 12U induced the strongest silencing of mutant allele (Figure 23A), with an inhibition of 95.6 ± 1.8% for the siRNA 9U, and 93.2 ± 2.3% for the siRNA 12U. Based on results obtained with R92Q allele silencing, additional siRNAs containing a single base mismatch were designed. siRNAs 9U(13U), 9U(14C), 9U(15U) were designed with the same sequence as siRNA 9U, except that carrying a base mismatch in the seed region (A>U, G>C and A>U in positions 13, 14 and 15, respectively). Similarly, siRNAs 12U(14C) and 12U(15U) were designed based on siRNA 12U sequence and including a single base mismatch in the seed region (G>C and A>U, respectively) (Figure 22A). Results of luciferase assay showed that the introduction of a single base mismatch resulted in a significant improvement of mutant allele silencing in comparison with the WT allele. In detail, among the five double mismatched siRNAs tested, the 12U(14C) induced a strong ASP-RNAi, determining an 87.4 ± 5.3% knockdown of R173W allele compared to a 39.9 ± 7.1% of silencing of the WT allele (Figure 23B).

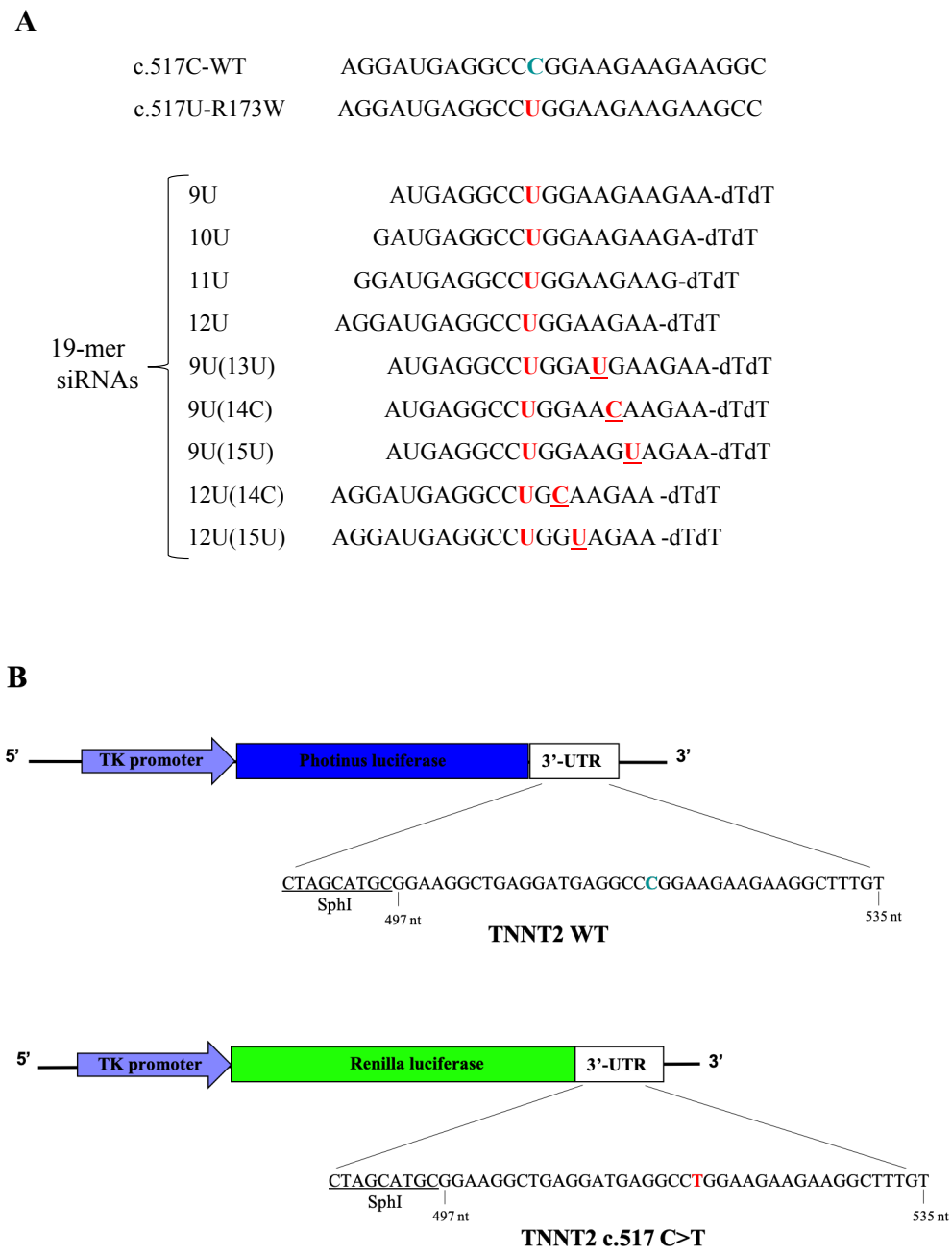

Figure 22. Design of siRNAs sequences and representation of reporter alleles. (A) Sequences of siRNAs duplex targeting R173W mutation: 19-mer sense-strand siRNAs with substitution nucleotide at position 9-12 and 19-mer sense-strand siRNAs (9U and 12U) carrying a single base mismatch. The nucleotide corresponding to the U mutation is shown in bold and red and the original C nucleotide is in bold and green. **(B)** Schematic maps of reporter alleles. Reporter alleles were constructed based on *Photinus* and *Renilla* luciferase genes transcribed starting from the TK promoter and containing in their 3'-UTR the sequences of the wild type or mutant alleles, respectively.

Nucleotides from +497 to +535 respect to the start codon refer to the human TNNT2 cDNA sequence (NM_001001430.3).

A

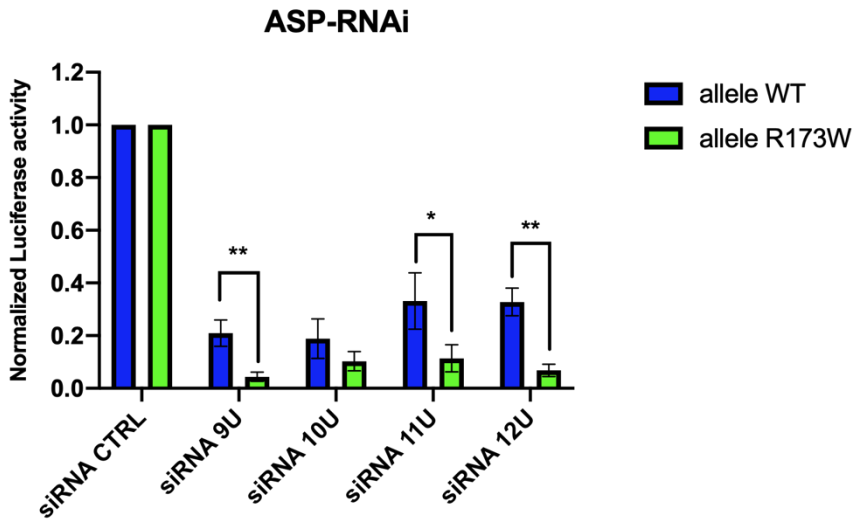

B

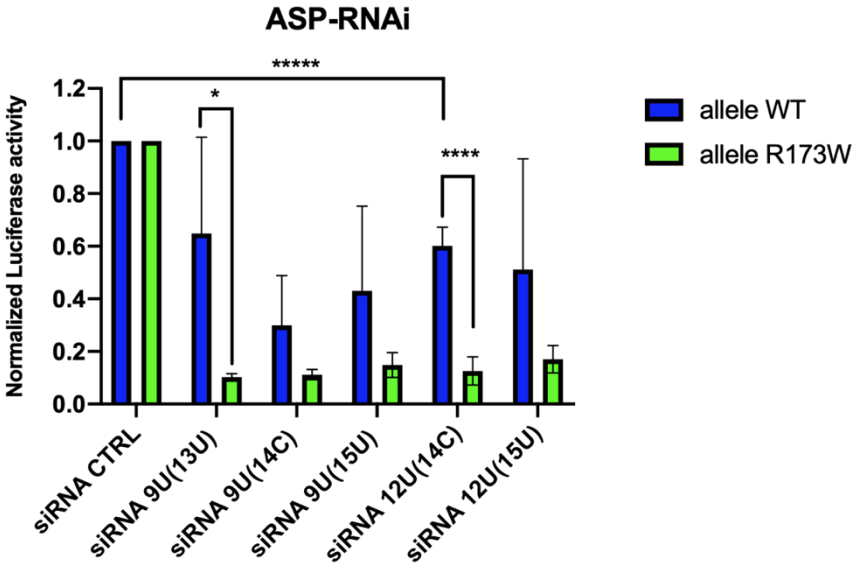

Figure 23. Assessment of ASP-RNAi on reporter alleles using 19-mer siRNAs (A) or 19-mer siRNA with a single nucleotide mismatch (B). Luciferase activity measured in HEK293T cells transfected with *Renilla* and *Photinus* luciferase expression plasmids. Luciferase levels were normalized against the levels of β-galactosidase activity. The β-galactosidase-normalized luciferase activity measured in the presence of siRNA duplexes were referred to the luciferase activity measured in the presence of

control siRNA. Data are presented as mean ± S.D. of four independent experiments (*p<0.05, **p<0.005, ****p<0.00005 and *****p<0.000005).

3.6 Analysis of ASP-RNAi on WT and mutant TNNT2 protein expression

To analyze the silencing effect of the selected siRNA on expression of wild-type and mutant TNNT2 proteins**,** HEK293T cells were co-transfected with expression plasmids for either wild type or mutant TNNT2 and siRNAs 12A(13U) and 12U(14C) targeting the R92Q and R173W mutant alleles, respectively.

The knockdown effect of siRNA 12A(13U) on the expression of the R92Q allele is shown in Figure 24. Transfection of HEK293T cells with the 12A(13U) siRNA resulted in a reduction of the expression of the R92Q TNNT2 protein of 88.8 ± 4.9% of compared to cells co-transfected with control siRNA or not co-transfected with any siRNA (Figure 24A, 24C). In addition, the expression level of the wild type allele was not significantly affected (104% of WT-TNNT2 expression in cells transfected with either siRNA 12A(13U) compared to 100% of WT-TNNT2 expression in control cell (-) (Figure 24D), indicating that the 12A(13U) siRNA may represent a good candidate for ASP-RNAi therapy. Similarly, western blot analysis of cells transfected with plasmid coding form the R173W TNNT2 protein showed that the 12U(14C) siRNA reduced the expression of the mutant protein of 92.7 ± 4.2% (Figure 25A, 25C). At difference with the 12A(13U) siRNA, however, the 12U(14C) siRNA also resulted in a significant reduction of the expression of wild type allele (Figure 25D).

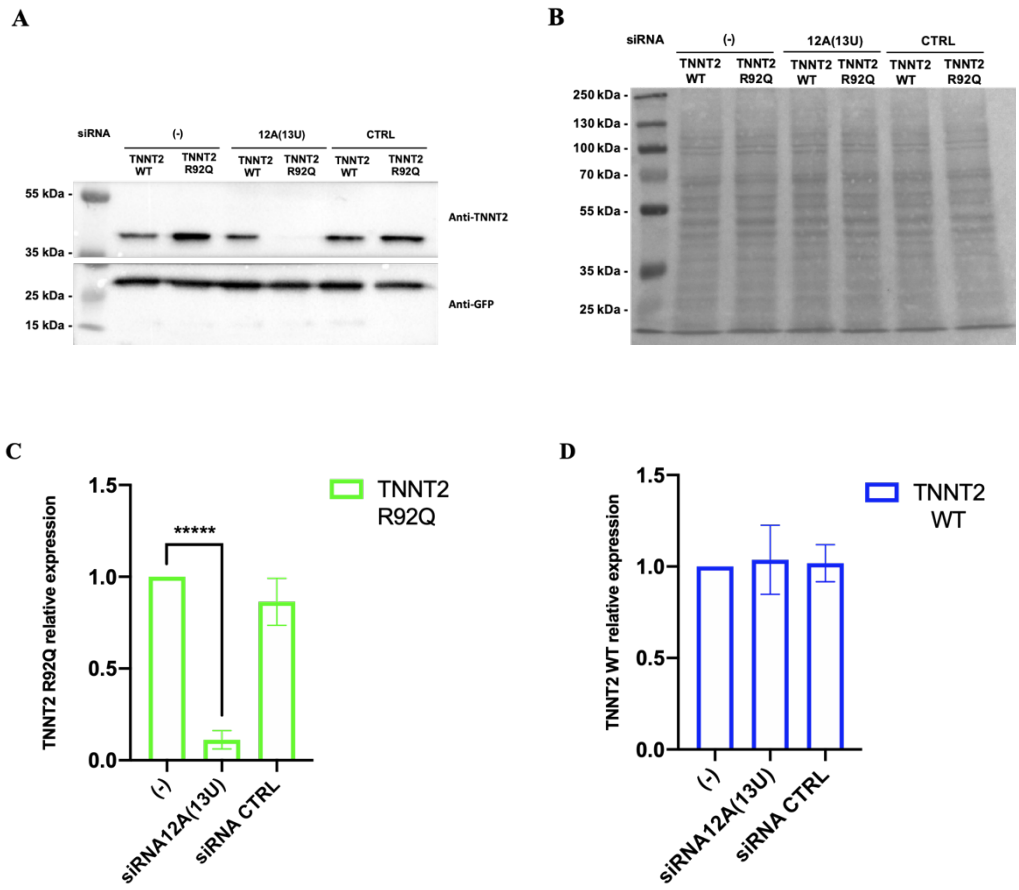

Figure 24. siRNA 12A(13U) specifically silences expression of R92Q TNNT2. (A) Western blot analysis of whole lysates of HEK293T cells co-transfected with expression plasmids coding for either WT or R92Q TNNT2 and control (CTRL) or 12A(13U) siRNA. Expression of TNNT2 was also evaluated in the absence of siRNA (-). One representative experiment of three is shown. **(B)** Ponceau-red staining of nitrocellulose membrane following protein transfer, related to western blot in (A), was shown as loading control. **(C)** R92Q TNNT2 relative expression in control cells (-) and in cells transfected with either siRNA 12A(13U) or control siRNA (CTRL). **(D)** WT TNNT2 relative expression in control cells (-) and in cells transfected with either siRNA 12A(13U) or control siRNA (CTRL). Protein expression levels were normalized to GFP. Data are presented as mean ± S.D. of three independent experiments (*****$p<0.000005$).

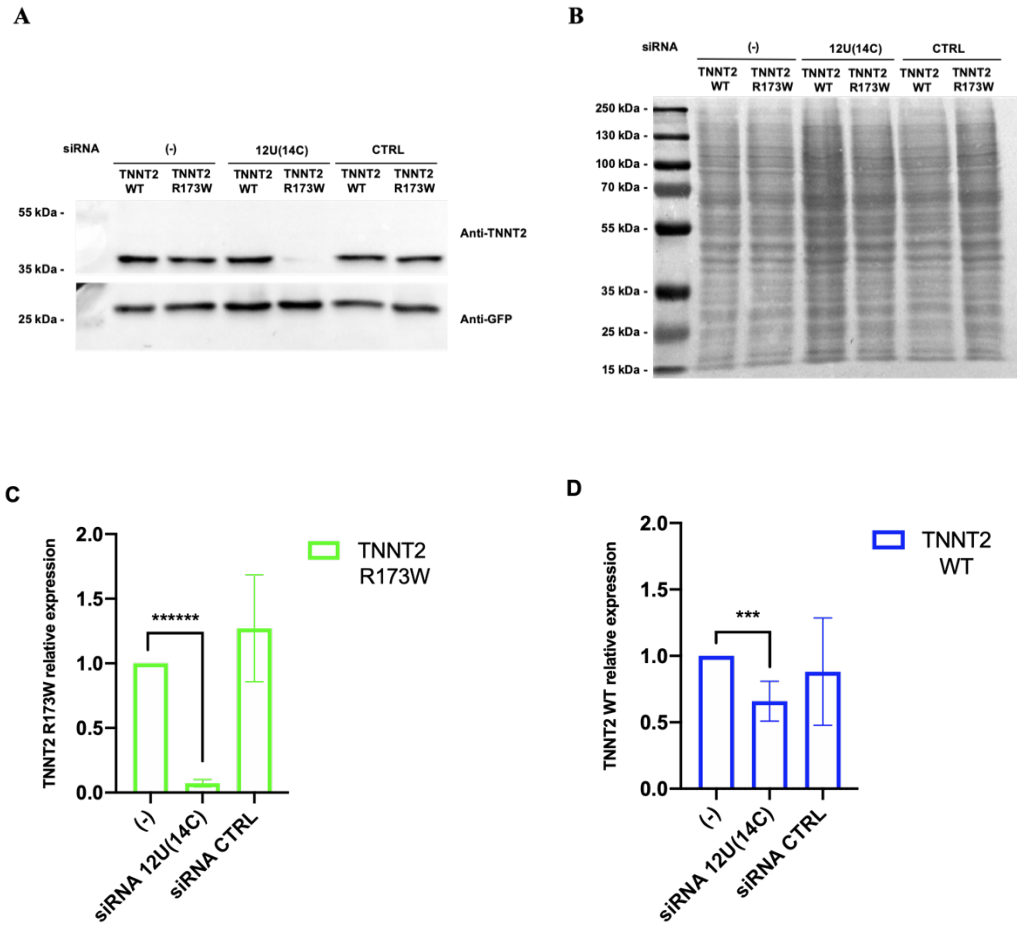

Figure 25. siRNA 12U(C14) specifically silences expression of R173W TNNT2. (A) Western blot analysis of whole lysates of HEK293T cells co-transfected cells co-transfected with expression plasmids coding for either WT or R173W TNNT2 and control (CTRL) or 12U(14C) siRNA. Expression of TNNT2 was also evaluated in the absence of siRNA (-). One representative experiment of three is shown. **(B)** Ponceau-red staining of nitrocellulose membrane following the protein transfer, related to western blot in (A), was shown as loading control. **(C)** TNNT2 R173W relative expression in control cells (-) and transfected with either siRNA 12U(14C) or control siRNA (CTRL). **(D)** WT TNNT2 relative expression in control cells (-) and in cells transfected with either siRNA 12U(14C) or control siRNA (CTRL). Protein expression levels were normalized to GFP. Data are presented as mean ± S.D. of three independent experiments (******p<0.0000005 and ***p<0.0005).

4. Discussion

Heterozygous dominant mutations in sarcomere proteins of the thick and thin filaments are the main genetic cause of HCM and DCM.

The cTnT sarcomere protein is the largest of the cTn complex and it mainly has a structural role. It is involved in the regulation of cardiac muscle contraction and is responsible in the association of the cTn complex with the thin filament and of the positioning of the other subunits in the complex (Perry SV, 1998). Most of DCM and HCM-causing mutations in *TNNT2* gene lead to the expression of mutant proteins that are incorporated in the sarcomere and affect the function and structure of the entire Tn complex, thus resulting in a dominant-negative effect (Lopes LR and Elliott PM, 2014). Mutations in *TNNT2* are highly clustered in the central and C-terminal region, involved in protein-protein interactions, specifically with the tropomyosin and the other cTn complex subunits (Marston SB, 2011).

Currently, the pharmacological intervention for HCM and DCM is mainly focused on symptoms relief and prevention of sudden cardiac death. In the last decades, several efforts have been done to develop therapeutic approaches for these patients, aimed to directly prevent the adverse effects of pathogenic mutations. Among them, the Allele-specific silencing by RNA interference (ASP-RNAi) represents a powerful and promising strategy to counteract genetic defects, targeting mutant alleles and leading to their degradation with minimal suppression of the corresponding wild-type alleles (Hohjoh H, 2013).

Significant therapeutic benefits have been demonstrated in iPSC-CM from patients and in mouse models treated with this approach, showing the recovery of structural integrity in cardiomyocytes and the cardiac contraction (Jiang J et al, 2013; Matsa E et al, 2014; Trochet D et al, 2018; Bongianino R et al, 2017).

In the present work, we developed a method for allele-specific gene silencing with siRNAs targeted to *TNNT2* c.275 G>A (p.R92Q) and c.517, C>T (p.R173W) mutations, identified in patients affected by HCM and DCM, respectively.

One of the most critical steps in ASP-RNAi, is siRNA design. Numerous studies suggested that siRNAs carrying nucleotide mutation at the central position had

the potential for conferring allele discrimination (Miller VM et al, 2004; Feng X et al, 2006; Huang H et al, 2009; Xia X et al, 2006; Sibley CR et al, 2006). It is therefore necessary to know the parameters to design siRNAs with high allele selectivity, especially when alleles differ at a single nucleotide. Usually, siRNAs duplexes are planned to have a sequence fully complementary to the mRNA target so that the endonuclease AGO2 of RISC complex is activated. Interestingly, AGO2 cleaves the mRNA target at the position corresponding to the center of the siRNA guide (between nucleotide positions 10 and 11 in a 20-mer RNA) (Ameres SL et al, 2007). Therefore, insertion the nucleotide mutation at the central position of siRNA is an important parameter to promote mRNA target cleavage. In case of dominant diseases due to point mutations, siRNAs will share a partial complementarity with the wild-type mRNA, that is characterized by only one base unpairing, making the cleavage less efficient.

We designed 19-21 nucleotide long siRNAs duplex carrying the mutant nucleotide in the central region; in detail, in the 19-mer siRNAs the mutant nucleotide was designed in positions from 9 to 12 (p9 to p12) and in the 21-mer siRNAs from p10 to p12. Moreover, siRNAs duplex were designed with two nucleotide overhangs at their 3'-end, (UU), that determine the asymmetry essential for the recognition and loading of siRNA guide into the RNAi machinery (Walton SP et al, 2010).

Firstly, we demonstrated that 19-mer siRNAs were able to inhibit the mutant allele more than the corresponding 21-mer siRNAs (Figure 20 and 21B) and that the ASP-RNAi was also largely affected by the position of mutation site into the siRNA sequence. siRNA carrying mutation at different positions were also analyzed by Trochet D *et al.* who demonstrated that position 9 and 12 were the most selective in silencing of the R465W mutant allele of DMN2 (Trochet D et al, 2018). Similarly to what observed in the assessment of p9 siRNA for the ASP-RNAi of *ALK2*-R206H mutation by Takahashi M *et al* and in the analysis of siRNA ranged from p9 to p12 reported by Ohnishi Y *et al* for the silencing of *PRNP*-D178N mutation (Ohnishi Y et al, 2008; Bongianino R et al, 2017; Takahashi M et al, 2012), our results show that the siRNAs carrying the mutant

nucleotide in a position between p9 and p12 are the most effective to silence the mutant TNNT2 alleles, but induce low or no allele discrimination.

In addition to the position, also the nature of nucleotide change might influence the siRNA efficacy. In this context, in a study by Du Q *et al* 20 siRNAs were tested against 400 target mismatches aiming to generate a model for single nucleotide-mismatch. It was demonstrated the existence of different tolerance levels of mismatches (Du Q et al, 2005). In detail, purine:purine or pyrimidine:pyrimidine base pairing between guide siRNA and mRNA are less tolerated, leading to the greatest level of discrimination compared to the purine:pyrimidine pairing, which is more tolerated. The formation of an A-form helix between the siRNA and mRNA target is required for mRNA cleavage and mismatches at or near the site of target cleavage. Several studies indicate that a greater structural distortion caused an optimal allele silencing activity, thus suggesting an explanation for some mutations to be more tolerated than others (Chiu YL and Rana TM, 2002; Huang H et al, 2009; Schwarz DS et al, 2006). Therefore, in our analysis of *TNNT2* ASP-RNAi, c.275 G>A (p.R92Q) and c.517, C>T (p.R173W) mutations are characterized by the change of a purine to a purine and pyrimidine to a pyrimidine, may lead to a tolerated purine:pyrimidine mismatch (G:U and C:A) in mRNA-siRNA interaction with the wild type alleles, thus explaining the low allele discrimination.

In order to enhance the ability of siRNAs to efficiently discriminate between mutant and wild type alleles we introduced some modifications in the siRNA sequence. In detail, we focused on the nucleotides 2-8 at the 5'-end of siRNA guide, corresponding to the seed region of miRNA. The seed region of miRNAs plays a key role in recognition of the 3'-UTR mRNA target, inducing the repression of translation (Lai EC, 2002). It was suggested that the 5'-end of siRNA guide can function as seed of miRNAs (Doench JG et al, 2003) and studies have shown that adding a mismatch in the seed region can improve the siRNA selectively and enhance the ASP-RNAi (Ohnishi Y et al, 2008; Chipman LB et al, 2019; Bartel DP, 2009; Humphreys DT et al, 2005; Takahashi M et al, 2012). Inclusion of a nucleotide mismatch into the seed region of siRNA

sequence actually induces one base unpairing between siRNA and mutant allele and two base unpairings between siRNA and wild type allele, resulting in an unstable interaction between the siRNA and the wild type allele, compared to the mutant allele. Therefore, the efficiency of silencing of the wild type mRNA and protein should be much lower than that of the mutant allele.

We designed three siRNAs targeting the c.275 G>A and four siRNA targeting the c.517 C>T mutation, carrying a mismatch into the seed region at different position. As showed in the luciferase assay analysis all the siRNAs carrying double mismatches improve the allele discrimination. However, not all double mismatched siRNAs analyzed conferred a strong ASP-RNAi, indicating that nucleotide position and the choice of the base substituted are critical aspects to be evaluated also in the design of double mismatched siRNAs.

In detail, siRNAs 12A(13U) and 12U(14C), targeting c.275 G>A (R92Q) and c.517 C>T (R173W) respectively, were shown to be the most efficient ones in inducing mutant allele knockdown. It's to note that, in siRNA 12A(13U) and the 12U(14C) carry the target mutation and the mismatch close one to each other (Figure 15 A), and divided by two and one nucleotides respectively compared to the other siRNAs targeting the correspondent mutation. Probably, this specific arrangement in the siRNA sequence, with the double mismatch occurring in a restricted region, results in the higher degree of destabilization of the wild type mRNA-siRNA pairing. These data are in agree with the ASP-RNAi of mismatched siRNAs obtained by Nogushi *et al* for *COL6A1*-G284R and Takahashi *et al* for *ALK2*-R206H, showing that the siRNA 12A(13U) enhances the ASP-RNAi compared to the no mismatched siRNA (Nogushi S et al, 2014; Takahashi M et al, 2012). The siRNA 12U(14C), at difference with the 12A(13U) siRNA targeting the R92Q mutation, induced a reduction in the expression of the wild type allele, indicating that extensive analysis of the knockdown potency of siRNAs duplexes by luciferase assay is required to select the most efficient and selective siRNA.

The analysis of ASP-RNAi efficiency on protein expression confirmed that both siRNA 12A(13U) and 12U(14C) are able to repress protein translation of the

mutant alleles with neither or minimal inhibition of wild-type allele. Further characterization will be performed on human iPS-derived cardiomyocytes.

In conclusion, our results showed that optimal allele discrimination was obtained with the use of siRNAs carrying a double-base mismatch both for the R92Q and the R173W mutation, indicating that the 12A(13U) and 12U(14C) siRNAs may represent good candidates for ASP therapy of HCM and DCM. Therefore, this study represents a good starting point for further exploration of knockdown of *TNNT2* mutations in *in vivo* models of cardiomyopathies.

5. Bibliography

Aartsma-Rus, A., Straub, V., Hemmings, R., Haas, M., Schlosser-Weber, G., Stoyanova-Beninska, V., Mercuri, E., Muntoni, F., Sepodes, B., Vroom, E., Balabanov, P. Development of exon skipping therapies for Duchenne muscular dystrophy: a critical review and a perspective on the outstanding issues. *Nucleic Acid Ther* 27:251-259.

Adams, D., Gonzalez-Duarte, A., O'Riordan, W.D, Yang, C.C., Ueda, M., Kristen, A.V., Tournev, I., Schmidt, H.H., Coelho, T., Berk, J.L., Lin, K.P., Vita, G., Attarian, S., Planté-Bordeneuve, V., Mezei, M.M., Campistol, J.M., Buades, J., Brannagan, T.H. 3rd, Kim, B.J., Oh J, Parman, Y., Sekijima, Y., Hawkins, P.N., Solomon, S.D., Polydefkis, M., Dyck, P.J., Gandhi, P.J., Goyal, S., Chen, J., Strahs, A.L., Nochur, S.V., Sweetser, M.T., Garg, P.P., Vaishnaw, A.K., Gollob, J.A., Suhr, O.B. Patisiran, an RNAi Therapeutic, for Hereditary Transthyretin Amyloidosis. *N Engl J Med.* 2018, 5;379(1):11-21.

Alcalai, R., Seidman, J.G., Seidman, C.E. Genetic basis of hypertrophic cardiomyopathy: from bench to the clinics. *Journal of cardiovascular electrophysiology*. 2008, 19:104-110.

Ameres, S.L., Martinez, J., Schroeder, R. Molecular basis for target RNA recognition and cleavage by human RISC. *Cell*. 2007, 130: 101-112.

Amoasii, L., Long, C., Li, H., Mireault, A.A., Shelton, J.M, Sanchez-Ortiz, E., McAnally, J.R., Bhattacharyya, S., Schmidt, F., Grimm, D., Hauschka, S.D., Bassel-Duby, R., Olson, E.N. Single-cut genome editing restores dystrophin expression in a new mouse model of muscular dystrophy. *Sci Transl Med. 2017,* 9(418):eaan8081.

Anderson, P.A., Greig, A., Mark, T.M., Malouf, N.N., Oakeley, A.E., Ungerleider, R.M., Allen, P.D., and Kay, B.K. Molecular basis of human cardiac troponin T isoforms expressed in the developing, adult, and failing heart. *Circulation Research.* 1995, 76:681-686.

Anderson, P.A.W, Malouf, N.N., Oakeley, A.E., Pagani, E.D., Allen. P.D. Troponin T isoform expression in humans. A comparison among normal and failing adult heart, fetal heart, and adult and fetal skeletal muscle. *Circulation Research*. 1991. 69:1226-1233.

Armani A, Galli S, Giacomello E, et al. Molecular interactions with obscurin are involved in the localization of muscle-specific small ankyrin1 isoforms to subcompartments of the sarcoplasmic reticulum. *Exp Cell Res*. 2006, 312(18):3546-3558.

Arbustini, E., Narula, N., Dec, G.W., Reddy, K.S., Greenberg, B., Kushwaha, S., Marwick, T., Pinney, S., Bellazzi, R., Favalli, V., Kramer, C., Roberts, R.,

Zoghbi, W.A., Bonow, R., Tavazzi, L., Fuster, V., Narula, J. The MOGE(S) classification for a phenotype-genotype nomenclature of cardiomyopathy: endorsed by the World Heart Federation. *J Am Coll Cardiol*. 2013, 62(22):2046-72.

Bagnato P, Barone V, Giacomello E, Rossi D, Sorrentino V. Binding of an ankyrin-1 isoform to obscurin suggests a molecular link between the sarcoplasmic reticulum and myofibrils in striated muscles. *J Cell Biol.* 2003,160(2):245-253.

Balke, C.W., Shorofsky, S.R. Alterations in calcium handling in cardiac hypertrophy and heart failure. *Cardiovascular Research.* 1998. 37(2):290-299.

Bartel DP. MicroRNAs: target recognition and regulatory functions. *Cell*. 2009, 136(2):215-33.

Basso, C., Corrado, D., Marcus, F.I., Nava, A., Thiene, G. Arrhythmogenic right ventricular cardiomyopathy. *Lancet.* 2009, 373(9671):1289-1300.

Baudenbacher, F., Schober, T., Pinto, J.R., Sidorov, V.Y., Hilliard, F., Solaro, R.J., Potter, J.D., Knollmann, B.C. Myofilament Ca2+ sensitization causes susceptibility to cardiac arrhythmia in mice. *J Clin Invest.* 2008, 118(12):3893-3903.

Ben Jehuda, R., Eisen, B., Shemer, Y., Mekies, L.N., Szantai, A., Reiter, I.,Cui, H., Guan, K., Haron-Khun, S., Freimark, D., Sperling, S.R., Gherghiceanu, M., Arad, M., Binah, O. CRISPR correction of the PRKAG2 gene mutation in the patient's induced pluripotent stem cell-derived cardiomyocytes eliminates electrophysiological and structural abnormalities. *Heart Rhythm.* 2018, 15:267-276.

Bernstein, E., Caudy, A.A., Hammond, S.M., Hannon, G.J. Role for a bidentate ribonuclease in the initiation step of RNA interference. *Nature.* 2001, 409:363-366.

Bers, D.M. Cardiac excitation–contraction coupling. *Nature.* 2002. 415(6868):198-205.

Bongianino, R., Denegri, M., Mazzanti, A., Lodola, F., Vollero, A., Boncompagni, S., Fasciano, S., Rizzo, G., Mangione, D., Barbaro, S., Di Fonso, A.; Napolitano, C., Auricchio, A., Protasi, F., Priori, SG. Allele-Specific Silencing of Mutant mRNA Rescues Ultrastructural and Arrhythmic Phenotype in Mice Carriers of the R4496C Mutation in the Ryanodine Receptor Gene (RYR2). *Circulation Research.* 2017, 121(5):525-536.

Braunwald, E. Cardiomyopathies An Overview. *Circulation Research*. 2017, 121:711-721.

Carrier, L., Knoll, R., Vignier, N., Keller, D.I., Bausero, P., Prudhon, B., Isnard, R., Ambroisine, M.L., Fiszman, M., Ross, J., Schwartz, K., Chien, K.R. Asymmetric septal hypertrophy in heterozygous cMyBP-C null mice. *Cardiovascular Research*. 2004, 63:293-304.

Chang, A.N., Harada, K., Ackerman, M.J., Potter, J.D. Functional consequences of hypertrophic and dilated cardiomyopathy-causing mutations in alphatropomyosin. *J Biol Chem.* 2005, 280(40):34343-34349.

Chipman LB, Pasquinelli AE. miRNA Targeting: Growing beyond the Seed. *Trends Genet*. 2019, 35(3):215-222.

Chiu, Y.L., Rana, T.M. siRNA function in RNAi: A chemical modification analysis. *RNA*. 2003, *9*(9):1034-1048.

Costa, F.F. Non-coding RNAs: lost in translation? *Gene*. 2007, 386(1-2):1-10.

Craig, R., Padrón, R. Molecular structure of the sarcomere. Textbook "Myology" (Editors A. G. Engel & C. Franzini-Armstrong), Third edition. McGraw-Hill. 2004. Chapter 7:129-166.

Cuccato G, Polynikis A, Siciliano V, Graziano M, di Bernardo M, di Bernardo D. Modeling RNA interference in mammalian cells. *BMC Syst Biol.* 2011, 27;5:19.

De Ynigo-Mojado, L.; Martin-Ruiz, I.; Sutherland, J.D. Efficient allele-specific targeting of LRRK2 R1441 mutations mediated by RNAi. *PLoS One.* 2011, 6(6): e21352.

Dec, G.W., Fuster, V. Idiopathic dilated cardiomyopathy. *N Engl J Med*. 1994, 331:1564-1575.

Doench, J.G., Petersen, C.P., Sharp, P.A. siRNAs can function as miRNAs. *Genes Dev*. 2003,17(4):438-42.

Dowler, T., Bergeron, D., Tedeschi, A.L., Paquet, L., Ferrari, N., Damha, M.J. Improvements in siRNA properties mediated by 2'-deoxy-2'-fluoro-beta-D-arabinonucleic acid (FANA). *Nucleic Acids Res.* 2006, *34*(6):1669–1675.

Du, Q., Thonberg, H., Wang, J., Wahlestedt, C., Liang, Z. A systematic analysis of the silencing effects of an active siRNA at all single-nucleotide mismatched target sites. *Nucleic Acids Res*. 2005, 33:1671–1677.

Ebashi, S., Ebashi, F., Kodama, A. Troponin as the Ca^{2+}-receptive Protein in the Contractile System. *The Journal of Biochemistry.* 1967, 62(1):137–138.

Elbashir, S.M., Martinez, J., Patkaniowska, A., Lendeckel, W., Tuschl, T. Functional anatomy of siRNAs for mediating efficient RNAi in Drosophila melanogaster embryo lysate. *EMBO J.* 2001, 20:6877–6888.

Elliott, P., Andersson, B., Arbustini, E., Bilinska, Z., Cecchi, F., Charron, P., Dubourg, O., Kühl, U., Maisch, B., McKenna, W.J., Monserrat, L., Pankuweit, S., Rapezzi, C., Seferovic, P., Tavazzi, L., Keren, A. Classification of the cardiomyopathies: a position statement from the European Society of Cardiology Working Group on Myocardial and Pericardial Diseases. *Eur Heart J.* 2008, 29(2):270-6.

Elmen, J., Thonberg, H., Ljungberg, K., Frieden, M., Westergaard, M., Xu, Y., Wahren, B., Liang, Z., Orum, H.; Koch, T.; Wahlestedt, C. Locked nucleic acid (LNA) mediated improvements in siRNA stability and functionality. *Nucleic Acids Res.* 2005, *33*(1):439-447.

Ervasti, J.M. Costameres: The Achilles' heel of Herculean muscle. *J Biol Chem*. 2003, 278(16):13591-13594.

Farza, H., Townsend, P.J., Carrier, L., Barton, P.J., Mesnard, L., Bahrend, E., Forissier, J.F., Fiszman, M., Yacoub, M.H., Schwartz, K. Genomic organisation, alternative splicing and polymorphisms of the human cardiac troponin T gene. *J Mol Cell Cardiol.* 1998, 30:1247-1253.

Feng, X.; Zhao, P.; He, Y.; Zuo, Z. Allele-specific silencing of Alzheimer's disease genes: The amyloid precursor protein genes with Swedish or London mutations. *Gene*. 2006, 371: 68–74.

Ferrantini, C., Coppini, R., Pioner, J.M., Gentile, F., Tosi, B., Mazzoni, L., Scellini, B., Piroddi, N., Laurino, A., Santini, L., Spinelli, V., Sacconi, L., De Tombe, P., Moore, R., Tardiff, J., Mugelli, A., Olivotto, I., Cerbai, E., Tesi, C., Poggesi, C. Pathogenesis of Hypertrophic Cardiomyopathy is Mutation Rather Than Disease Specific: A Comparison of the Cardiac Troponin T E163R and R92Q Mouse Models. *J Am Heart Assoc.* 2017, 6(7):e005407.

Fifer, M.A., Vlahakes, G.J. Management of symptoms in hypertrophic cardiomyopathy. *Circulation.* 2008, 117(3):429-39.

Fire, A., Xu, S., Montgomery, M.K., Kostas, S.A., Driver, S.E., Mello, C.C. Potent and specific genetic interference by double-stranded RNA in Caenorhabditis elegans. *Nature.* 1998, 391:806-811.

Fujino, N., Shimizu, M., et al. A novel mutation Lys273Glu in the cardiac troponin T gene shows high degree of penetrance and transition from hypertrophic to dilated cardiomyopathy. *Am J Cardiol.* 2002, 89(1):29-33.

Gautel, M., Djinović-Carugo, K. The sarcomeric cytoskeleton: from molecules to motion. *J Exp Biol*. 2016, 219(2):135-145.

Gersh, B.J., Maron, B.J., Bonow, R.O., et al. ACCF/AHA guideline for the diagnosis and treatment of hypertrophic cardiomyopathy: a report of the American College of Cardiology Foundation/American Heart Association Task Force on Practice Guidelines. *Circulation*. 2011; 124(24): e783-e831.

Gerull, B., Gramlich, M., Atherton, J. et al. Mutations of TTN, encoding the giant muscle filament titin, cause familial dilated cardiomyopathy. *Nat Genet.* 2002, 30:201-204.

Golob, M., Moss, R.L., Chesler, N.C. Cardiac tissue structure, properties, and performance: a materials science perspective. *Ann Biomed Eng*. 2014, 42(10):2003-13.

Gomes, A.V., Potter, J.D., Szczesna-Cordary, D. The role of troponins in muscle contraction. *IUBMB Life.* 2002, 54(6):323-33.

Hammond, S.M., Wood, M.J. Genetic therapies for RNA missplicing diseases. *Trends Genet. 2011,* 27:196-205.

Hanna, E., Remuzat, C., Auquier, P., Toumi, M. Gene therapies development: slow progress and promising prospect. *J Mark Access Health Policy.* 2007, 5:1265293.

Harada, K., Potter, J.D. Familial hypertrophic cardiomyopathy mutations from different functional regions of troponin T result in different effects on the pH and Ca^{2+} sensitivity of cardiac muscle contraction. *J Biol Chem*. 2004, 279(15):14488-14495.

Harada, K., Potter, J.D. Familial hypertrophic cardiomyopathy mutations from different functional regions of troponin T result in different effects on the pH and Ca2+ sensitivity of cardiac muscle contraction. *J Biol Chem.* 2004, 279(15):14488-14495.

Herman, D.S., Lam, L., Taylor, M.R., Wang, L., Teekakirikul, P., Christodoulou, D., Conner, L., et al. Truncations of titin causing dilated cardiomyopathy. *N Engl J Med.* 2012, 366(7):619-628.

Hershberger, R.E., Pinto, J.R., Parks, S.B., Kushner, J.D., Li D., et al. Clinical and functional characterization of tnnt2 mutations identified in patients with dilated cardiomyopathy. *Circulation Cardiovascular Genetic*. 2009, 2:306-313.

Hershberger, R.E., Pinto, J.R., Parks, S.B., Kushner, J.D., Li, D., Ludwigsen, S., Cowan, J., Morales, A., Parvatiyar, M.S., Potter, J.D. Clinical and functional

characterization of TNNT2 mutations identified in patients with dilated cardiomyopathy. *Circulation Cardiovascular Genetics*. 2009, 2:306-313.

Hirai, H., Satoh, E., Osawa, M., Inaba, T., Shimazaki, C., Kinoshita, S., Nakagawa, M., Mazda, O., Imanishi, J. Use of EBV-based vector/ HVJ-liposome complex vector for targeted gene therapy of EBV-associated neoplasms. *Biochem Biophys Res Commun.* 1997, 241:112-118.

Ho, S.N., Hunt, H.D., Horton, R.M., Pullen, J.K., Pease, L.R. Site-directed mutagenesis by overlap extension using the polymerase chain reaction. *Gene.* 1989, 77(1):51-9.

Hohjoh, H. Allele-specific silencing by RNA interference. *Methods Mol. Biol*. 2010, *623*:67-79.

Hohjoh, H. Disease-causing allele-specific silencing by RNA interference. *Pharmaceuticals (Basel)*. 2013, 6(4):522-35.

Hong, T., Shaw, R.M. Cardiac T-Tubule Microanatomy and Function. *Physiol Rev.* 2017, 97(1): 227-252.

Howarth, J. W., Meller, J., Solaro, R. J., Trewhella, J., and Rosevear, P. R. Phosphorylation-dependent conformational transition of the cardiac specific N-extension of troponin I in cardiac troponin. *J. Mol. Biol.* 2007, 373(3):706-722.

Hsu, P.D., Lander, E.S., Zhang, F. Development and applications of CRISPR-Cas9 for genome engineering. *Cell.* 2014, 157:1262-1278.

Hsu, D.T., Canter, C.E. Dilated cardiomyopathy and heart failure in children. *Heart Fail Clin.* 2010, 6(4):415-32.

Huang, H., Qiao, R., Zhao, D., Zhang, T., Li, Y., Yi, F., Lai, F., Hong, J., Ding, X., Yang, Z., Zhang L., Du, L., Liang, Z. Profiling of mismatch discrimination in RNAi enabled rational design of allele-specific siRNAs. *Nucleic Acids Res.* 2009, 37(22):7560-7569.

Humphreys, D.T., Westman, B.J., Martin, D.I., Preiss, T. MicroRNAs control translation initiation by inhibiting eukaryotic initiation factor 4E/cap and poly(A) tail function. *Proc Natl Acad Sci U S A.* 2005, 102(47):16961-6.

Huxley, A.F., and R. Niedergerke. Structural changes in muscle during contraction. Nature. 1954, 173:971-973.

Ikeda, U., Minamisawa, M., Koyama, J. Isolated left ventricular noncompaction cardiomyopathy in adults. *J Cardiol*. 2015, 65(2): 91-97.

Itoh-Satoh, M., Hayashi, T., Nishi, H., Koga, Y., Arimura, T., Koyanagi, T., Takahashi, M., Hohda, S., Ueda, K., Nouchi, T., Hiroe, M., Marumo, F., Imaizumi, T., Yasunami, M., Kimura, A. Titin mutations as the molecular basis for dilated cardiomyopathy. *Biochem Biophys Res Commun.* 2002, 291(2):385-393.

Jackson, A.L., Linsley, P.S. Recognizing and avoiding siRNA off-target effects for target identification and therapeutic application. *Nature Reviews Drug Discovery.* 2010, 9(1):57-67.

Jaski, B.E, Jessup, M.L., Mancini, D.M., Cappola, T.P., Pauly, D.F., Greenberg, B., Borow, K., Dittrich, H., Zsebo, K.M., Hajjar, R.J. Calcium upregulation by percutaneous administration of gene therapy in cardiac disease (CUPID trial), a first-in-human phase ½ clinical trial. *J Card Fail.* 2009, 15:171-181.

Jiang, J., Wakimoto, H., Seidman, J.G., Seidman, C.E. Allele specific silencing of mutant Myh6 transcripts in mice suppresses hypertrophic cardiomyopathy. *Science*. 2013, 342:111-114.

Jinek, M., Chylinski, K., Fonfara, I., Hauer, M., Doudna, J.A., Charpentier, E. A programmable dual-RNA-guided DNA endonuclease in adaptive bacterial immunity. *Science.* 2012, 337:816-821.

Junqueira, L.C., and J. Carneiro. Basic histology text and atlas. London: McGraw Hill. 2005.

Kamisago, M., Sharma, S.D., DePalm,a S.R., Solomon, S., Sharma, P., McDonough, B., Smoot, L., Mullen, M.P., Woolf, P.K., Wigle, E.D., Seidman, J.G., Seidman, C.E. Mutations in sarcomere protein genes as a cause of dilated cardiomyopathy. *N Engl J Med.* 2000, 343(23):1688-1696.

Katrukha, I.A. Human cardiac troponin complex. Structure and functions. *Biochemistry*. 2013, 78(13):1447-65.

Kim, T.K., Eberwine, J.H. Mammalian cell transfection: the present and the future. *Anal Bioanal Chem.* 2010, 397:3173-8.

Knöll, R., Hoshijima, M., Hoffman, H.M., Person, V., Lorenzen-Schmidt, I., Bang, M.L., Hayashi, T., Shiga, N., Yasukawa, H., Schaper, W., McKenna, W., Yokoyama, M., Schork, N.J., Omens, J.H., McCulloch, A.D., Kimura, A., Gregorio, C.C., Poller, W., Schaper, J., Schultheiss, H.P., Chien, K.R. The cardiac mechanical stretch sensor machinery involves a Z disc complex that is defective in a subset of human dilated cardiomyopathy. *Cell.* 2002, 111(7): 943-955

Krendel, M., Mooseker, M.S. Myosins: Tails (and Heads) of Functional Diversity Myosins: Tails (and Heads) of Myosin Superfamily: Diversity of. *Physiology*. 2006, 239-251.

Kretsinger, R. H. Structure and evolution of calcium-modulated proteins. *CRC Crit. Rev. Biochem.* 1980, 8(2):119-174.

Kretsinger, R.H., Nockolds, C.E. Carp muscle calcium-binding protein. II. Structure determination and general description. *J Biol Chem*. 1973, 248(9):3313-26.

Kulikovskaya, I., McClellan, G., Levine, R., Winegrad, S. Effect of extraction of myosin binding protein C on contractility of rat heart. *Am J Physiol Heart Circ Physiol.* 2003, 285:H857-H865.

Labeit, S., Barlow, D.P., Gautel, M., Gibson, T., Holt, J., Hsieh, C.L., Francke, U., Leonard, K., Wardale, J., Whiting, A., et al. A regular pattern of two types of 100-residue motif in the sequence of titin. *Nature.* 1990, 345(6272):273-6.

Lai, E.C. Micro RNAs are complementary to 3'UTR sequence motifs that mediate negative post-transcriptional regulation. *Nature Genetics.* 2002, 30: 363-364.

Lakdawala, N.K., Dellefave, L., Redwood, C.S., Sparks, E., Cirino, A.L., Depalma, S., Colan, S.D., Funke, B., Zimmerman, R.S., Robinson, P., Watkins, H., Seidman, C.E., Seidman, J.G., McNally, E.M., Ho, C.Y. Familial dilated cardiomyopathy caused by an alpha-tropomyosin mutation: the distinctive natural history of sarcomeric dilated cardiomyopathy. *J Am Coll Cardiol*. 2010, 55(4):320-329.

Lange, S., Ouyang, K., Meyer, G., et al. Obscurin determines the architecture of the longitudinal sarcoplasmic reticulum. *J Cell Sci*. 2009, 122(15):2640-2650.

Li, D., Czernuszewicz, G.Z., Gonzalez, O., Tapscott, T., Karibe, A., Durand, J.B, Brugada, R., Hill, R., Gregoritch, J.M., Anderson, J.L., Quiñones, M., Bachinski, L.L., Roberts, R. Novel cardiac troponin T mutation as a cause of familial dilated cardiomyopathy. *Circulation.* 2001, 104(18):2188-2193.

Li, M. X., Spyracopoulos, L., and Sykes, B. D. Binding of cardiac troponin I 147-163 induces a structural opening in human cardiac troponin-C. *Biochemistry*.1999, 38(26):8289-8298.

Li, M.X., Hwang, P.M. Structure and Function of Cardiac Troponin C (TNNC1): Implications for Heart Failure, Cardiomyopathies, and Troponin Modulating Drugs. *Gene.* 2015, 571(2): 153-166.

Linden, R. Gene therapy: what it is, what it is not and what it will be. *Estud Av.* 2010, 24(70):31-69.

Lopes, L.R., Elliott, P.M. A straightforward guide to the sarcomeric basis of cardiomyopathies. *Heart.* 2014, 100(24):1916-23.

Luk, A., Ahn, E., Soor, G.S., Butany, J. Dilated cardiomyopathy: a review. *J Clin Pathol.* 2009, 62(3): 219-225.

Ma, H., Marti-Gutierrez, N., Park, S.W., Wu, J., Lee, Y., Suzuki, K., Koski, A., Ji, D., Hayama, T., Ahmed, R., Darby, H., Van, Dyken C., Li, Y., Kang, E., Park, A.R., Kim, D., Kim, S.T., Gong, J., Gu, Y., Xu, X., Battaglia, D., Krieg, S.A., Lee, D.M., Wu, D.H., Wolf, D.P., Heitner, S.B., Belmonte, JCI, Amato, P., Kim, J.S., Kaul, S., Mitalipov, S. Correction of a pathogenic gene mutation in human embryos. *Nature. 2017,* 548:413-419.

Malnic, B., Farah, C.S., Reinach, F.C. Regulatory properties of the NH2- and COOH-terminal domains of troponin T. ATPase activation and binding to troponin I and troponin C. *J Biol Chem*. 1998, 273(17):10594-601.

Manning, E.P., Guinto, P.J., Tardiff, J.C. Correlation of molecular and functional effects of mutations in cardiac troponin T linked to familial hypertrophic cardiomyopathy: an integrative in silico/in vitro approach. *The Journal of biological chemistry*. 2012, 287:14515-14523.

Maron, B.J., Gardin, J.M., Flack, J.M., Gidding, S.S., Kurosaki, T.T., Bild, D.E. Prevalence of hypertrophic cardiomyopathy in a general population of young adults. Echocardiographic analysis of 4111 subjects in the CARDIA Study. Coronary Artery Risk Development in (Young) Adults. *Circulation*. 1995, 92:785-789.

Maron, B.J., Maron, M.S. Hypertrophic cardiomyopathy. *Lancet*. 2013, 381:242-255.

Maron, B.J., Maron, M.S., Semsarian, C. Genetics of hypertrophic cardiomyopathy after 20 years: clinical perspectives. *J Am Coll Cardiol.* 2012, 60(8):705-15.

Maron, B.J., Towbin, J.A., Thiene, G., Antzelevitch, C., Corrado, D., Arnett, D., Moss, A.J., Seidman, C.E., Young, J.B. Contemporary definitions and classification of the cardiomyopathies: an American Heart Association Scientific Statement from the Council on Clinical Cardiology, Heart Failure and Transplantation Committee; Quality of Care and Outcomes Research and Functional Genomics and Translational Biology Interdisciplinary Working Groups; and Council on Epidemiology and Prevention. *Circulation*. 2006, 113(14):1807-1816.

Marston, S., Copeland, O., Jacques, A., Livesey, K., Tsang, V., McKenna, W.J., Jalilzadeh, S., Carballo, S., Redwood, C., Watkins, H. Evidence from human

myectomy samples that MYBPC3 mutations cause hypertrophic cardiomyopathy through haploinsufficiency. *Circulation Research.* 2009, 105:219-222.

Marston, S.B. How Do Mutations in Contractile Proteins Cause the Primary Familial Cardiomyopathies? *Journal of Cardiovascular Translational Research*. 2011, 4:245-255.

Masarone, D., Kaski, J.P., Pacileo, G., Elliott, P.M., Bossone, E., Day, S.M., Limongelli, G. Epidemiology and Clinical Aspects of Genetic Cardiomyopathies. *Heart Fail Clin.* 2018, 14(2):119-128.

Matsa, E., Dixon, JE., Medway, C., Georgiou, O., Patel, MJ., Morgan, K., Kemp, PJ., Staniforth, A., Mellor, I., Denning, C. Allele-specific RNA interference rescues the long-QT syndrome phenotype in human-induced pluripotency stem cell cardiomyocytes. *European Heart Journal*. 2014, 35(16):1078-87.

McConnell, M., Tal Grinspan, L., Williams, M.R., Lynn, M.L., Schwartz, B.A., Fass, O.Z., Schwartz S.D., Tardiff, J.C. Clinically Divergent Mutation Effects on the Structure and Function of the Human Cardiac Tropomyosin Overlap. *Biochemistry.* 2017, 56(26):3403-3413.

McElhinny, A.S., Kazmierski S.T., Labeit, S. and Gregorio C.C. Nebulin: the nebulous, multifunctional giant of striated muscle. *Trends in cardiovascular medicine.* 2003, 13:195-201.

McNally, E.M., Golbus, J.R. and Puckelwartz, M.J. Genetic mutations and mechanisms in dilated cardiomyopathy. *The Journal of Clinical Investigation.* 2013, 123(1).

Mearini, G., Stimpel, D., Kramer, E., Geertz, B., Braren, I., Gedicke-Hornung, C., Precigout, G., Muller, O.J., Katus, H.A., Eschenhagen, T., Voit, T., Garcia, L., Lorain, S., Carrier, L. Repair of Mybpc3 mRNA by 5′-trans-splicing in a mouse model of hypertrophic cardiomyopathy. *Mol Ther Nucleic Acids.* 2013, 2:e102.

Mesnard, L., Logeart, D., Taviaux, S., Diriong, S., Mercadier, J. J., and Samson, F. Human Cardiac Troponin T: Cloning and Expression of New Isoforms in the Normal and Failing Heart. *Circulation Research.* 1995, 76(4):687-692.

Miller, V.M.; Gouvion, C.M.; Davidson, B.L.; Paulson, H.L. Targeting Alzheimer's disease genes with RNA interference: An efficient strategy for silencing mutant alleles. *Nucleic Acids Res.* 2004, 32: 661-668.

Mirza, M., Marston, S., Willott, R., Ashley, C., Mogensen, J., McKenna, W., Robinson, P., Redwood, C., Watkins, H. Dilated cardiomyopathy mutations in

three thin filament regulatory proteins result in a common functional phenotype. *J Biol Chem.* 2005, 280(31):28498-28506.

Mogensen, J., Murphy, R.T., Shaw, T., Bahl, A., Redwood, C., Watkins, H., Burke, M., Elliott, P.M., McKenna, W.J. Severe disease expression of cardiac troponin C and T mutations in patients with idiopathic dilated cardiomyopathy. *J Am Coll Cardiol*. 2004, 44(10):2033-2040.

Mogensen, J., Murphy, R.T., Shaw, T., Bahl, A., Redwood, C., Watkins, H., Burke, M., Elliott, P.M., McKenna, W.J. Severe disease expression of cardiac troponin C and T mutations in patients with idiopathic dilated cardiomyopathy. *J Am Coll Cardiol*. 2004, 44(10):2033-2040.

Morimoto, S.; Yanaga, F.; Minakami, R.; Ohtsuki, I. Ca2+-sensitizing effects of the mutations at Ile-79 and Arg-92 of troponin T in hypertrophic cardiomyopathy. *Am J Physiol*. 1998, 275(1):C200-7.

Morimoto, S. Molecular pathogenic mechanisms of cardiomyopathies caused by mutations in cardiac troponin t. *Advances in experimental medicine and biology*. 2007, 592:227-239.

Morimoto, S. Sarcomeric proteins and inherited cardiomyopathies. *Cardiovascular Research*. 2008, 77(4):659-666.

Muchtar, E., Blauwet, L.A., Gertz, M.A. Restrictive Cardiomyopathy: Genetics, Pathogenesis, Clinical Manifestations, Diagnosis, and Therapy. *Circulation Research*. 2017, 121(7):819-837.

Nakaura, H., Yanaga, F., Ohtsuki, I., Morimoto, S. Effects of missense mutations Phe110Ile and Glu244Asp in human cardiac troponin T on force generation in skinned cardiac muscle fibers. *J Biochem.* 1999, 126(3):457-460.

Narula, N., Favalli, V., Tarantino, P., Grasso, M., Pilotto, A., Bellazzi, R., Serio, A., Gambarin, F.I., Charron, P., Meder, B., Pinto, Y., Elliott, P.M., Mogensen, J., Bolognesi, M., Bollati, M., Nayerossadat, N., Maedeh, T., Ali, P.A. Viral and non-viral delivery systems for gene delivery. *Adv Biomed Res.* 2012, 1:27.

Nihoyannopoulos, P., Dawson, D. Restrictive cardiomyopathies. *Journal of Echocardiography*. 2009, 10(8):iii23-33.

Noguchi, S., Ogawa, M., Kawahara, G., Malicdan, M.C., Nishino, I. Allele-specific Gene Silencing of Mutant mRNA Restores Cellular Function in Ullrich Congenital Muscular Dystrophy Fibroblasts. *Mol Ther Nucleic Acids.* 2014, 3(6):e171.

Norton, N., Li, D., Rampersaud, E., Morales, A., Martin, E.R., Zuchner, S., Guo, S., Gonzalez, M., Hedges, D.J., Robertson, P.D., Krumm, N., Nickerson, D.A.,

Hershberger, R.E. Exome sequencing and genomewide linkage analysis in 17 families illustrate the complex contribution of TTN truncating variants to dilated cardiomyopathy. *Circ Cardiovasc Genet.* 2013, 6(2):144-153.

Oakley, C.E., Hambly, B.D., Curmi, P.M., Brown, L.J. Myosin binding protein C: structural abnormalities in familial hypertrophic cardiomyopathy. *Cell research.* 2004, 14: 95-110.

Oberst, L., Zhao, G., Park, J.T., Brugada, R., Michael, L.H., Entman, M.L., Roberts, R., Marian, A.J. Dominant-negative Effect of a Mutant Cardiac Troponin T on Cardiac Structure and Function in Transgenic Mice. *J. Clin. Invest.* 1998, 102:1498-1505.

Ohnishi, Y., Tamura, Y., Yoshida, M., Tokunaga, K., Hohjoh, H. Enhancement of allele discrimination by introduction of nucleotide mismatches into siRNA in allele-specific gene silencing by RNAi. *PLoS One.* 2008, 3(5):e2248.

Ohtsuki, I. Molecular arrangement of troponin-T in the thin filament. *Journal of Biochemistry.* 1979, 86:491-497.

Palm, T., Graboski, S., Hitchcock-DeGregori, S.E., Greenfield, N.J. Disease-causing mutations in cardiac troponin T: identification of a critical tropomyosin-binding region. *Biophys J.* 2001, 81(5):2827-37.

Pappas, C.T., Bliss, K.T., Zieseniss, A., Gregorio, C.C. The Nebulin family: an actin support group. *Trends in cell biology.* 2011, 21:29-37.

Parmacek, M.S., Solaro, R.J. Biology of the troponin complex in cardiac myocytes. *Prog Cardiovasc Dis*. 2004, 47(3):159-76.

Perry, S.V. Troponin T: genetics, properties and function. *Muscle Research Cell Motility*. 1998, 19(6):575-602.

Perry, S.V. Vertebrate tropomyosin: distribution, properties and function. *Journal of Muscle Research and Cell Motility.* 2001, 22:5-49.

Potter, J. D., and Gergely, J. The calcium and magnesium binding sites on troponin and their role in the regulation of myofibrillar adenosine triphosphatase. *J. Biol. Chem.* 1975, 250(12):4628-4633.

Prondzynski, M., Kramer, E., Laufer, S.D., Shibamiya, A., Pless, O., Flenner, F., Muller, O.J., Munch, J., Redwood, C., Hansen, A., Patten, M., Eschenhagen, T., Mearini, G., Carrier, L. Evaluation of MYBPC3 trans-splicing and gene replacement as therapeutic options in human iPSC-derived cardiomyocytes. *Mol Ther Nucleic Acids*. 2017, 7:475-486.

Prondzynski, M., Mearini, G., Carrier, L. Gene therapy strategies in the treatment of hypertrophic cardiomyopathy. *Pflugers Arch.* 2019, 471(5):807-815.

Pugh, T.J., Kelly, M.A., Gowrisankar, S., Hynes, E., Seidman, M.A., Baxter, S.M., Bowser, M., Harrison, B., Aaron, D., Mahanta, L.M., Lakdawala, N.K., McDermott, G., White, E.T., Rehm, H.L., Lebo, M., Funke, B.H. The landscape of genetic variation in dilated cardiomyopathy as surveyed by clinical DNA sequencing. *Genet Med.* 2014, 16(8):601-608.

Randazzo, D., Giacomello, E., Lorenzini, S., Rossi, D., Pierantozzi, E., Blaauw, B., Reggiani, C., Lange, S., Peter, A.K., Chen, J., Sorrentino, V. Obscurin is required for ankyrinB-dependent dystrophin localization and sarcolemma integrity. *J Cell Biol*. 2013, 200(4):523-536.

Reich, S.J., Fosnot, J., Kuroki, A., Tang, W., Yang, X., Maguire, A.M., Bennett, J., Tolentino, M.J. Small interfering RNA (siRNA) targeting VEGF effectively inhibits ocular neovascularization in a mouse model. *Mol Vis*. 2003, 9:210-216.

Repetti, G.G., Toepfer, C.N., Seidman, J.G., Seidman, C.E. Novel Therapies for Prevention and Early Treatment of Cardiomyopathies. *Circulation Research.* 2019, 124(11):1536-1550.

Robinson, P., Griffiths, P. J., Watkins, H., & Redwood, C. S. Dilated and hypertrophic cardiomyopathy mutations in troponin and alpha-tropomyosin have opposing effects on the calcium affinity of cardiac thin filaments. *Circulation Research*. 2007, 101(12):1266-1273.

Rosol, M., Lehman, W., Craig, R., Landis, C., Butters, C., Tobacman, L.S. Three-dimensional reconstruction of thin filaments containing mutant tropomyosin. *Biophys J*. 2000, 78(2):908-917.

Ross M. & Pawlina W. Istologia. Teste e atlante. Con elementi di biologia cellulare e molecolare. CEA editore. 2016.

Rossi, D., Barone, V., Giacomello, E., Cusimano, V., Sorrentino, V. The sarcoplasmic reticulum: an organized patchwork of specialized domains. *Traffic.* 2008, 9(7):1044-9.

Sabry, M.A., Dhoot, G.K. Identification of and changes in the expression of troponin T isoforms in developing avian and mammalian heart. *Journal of Molecular and Cellular Cardiology.* 1989, 21(1):85-91.

Sadayappan, S., Finley, N., Howarth, J.W., Osinska, H., Klevitsky, R., Lorenz, J.N., Rosevear, P.R., Robbins, J. Role of the acidic N' region of cardiac troponin I in regulating myocardial function. *The FASEB Journal.* 2008, 22(4):1246-1257.

Sandow, A. Excitation-contraction coupling in skeletal muscle. *Pharmacology Review.* 1965, 17(3):265-320.

Saxena, S, Jónsson, ZO and Dutta, A. Small RNAs with imperfect match to endogenous mRNA repress translation. Implications for off-target activity of small inhibitory RNA in mammalian cells. *J Biol Chem*. 2003, 278: 44312-44319.

Schmitt, J.P., Debold, E.P., Ahmad, F., Armstrong, A., Frederico A, Conner, D.A. Mende, U., Lohse, M.J., Warshaw, D., Seidman, C.E., Seidman, J.G. Cardiac myosin missense mutations cause dilated cardiomyopathy in mouse models and depress molecular motor function. *Proc Natl Acad Sci USA*. 2006, 103(39):14525-14530.

Schwartz, K., Mercadier, J.J. Cardiac troponin T and familial hypertrophic cardiomyopathy: an energetic affair. *J Clin Invest*. 2003, 112(5):652-654.

Schwarz, D.S.; Ding, H.; Kennington, L.; Moore, J.T.; Schelter, J.; Burchard, J.; Linsley, P.S.; Aronin, N.; Xu, Z.; Zamore, P.D. Designing siRNA that distinguish between genes that differ by a single nucleotide. *PLoS Genet*. 2006, 2(9):e140.

Scriven, D.R., Asghari, P., Moore, ED. Microarchitecture of the dyad. *Cardiovasc Research*. 2013. 98(2):169-76.

Seidman, C.E., Seidman, J.G. Identifying sarcomere gene mutations in hypertrophic cardiomyopathy: a personal history. *Circulation Research*. 2011, 108:743-50.

Sevrieva, I., Knowles, A.C., Kampourakis, T., Sun, Y.B. Regulatory domain of troponin moves dynamically during activation of cardiac muscle. *J Mol Cell Cardiol*. 2014, 75:181-7.

Sibley, C.R., Wood, M.J. Identification of allele-specific RNAi effectors targeting genetic forms of Parkinson's disease. *PLoS One.* 2011, 6(6):e26194.

Squire, J.M. Architecture and function in the muscle sarcomere. *Current opinion in structural biology*. 1997, 7:247-257.

Sun, N., Yazawa, M., Liu, J., Han, L., Sanchez-Freire, V., Abilez, O.J., Navarrete, E.G., Hu, S., Wang, L., Lee, A., Pavlovic, A., Lin, S., Chen, R., Hajjar, R.J., Snyder, M.P., Dolmetsch, R.E., Butte, M.J., Ashley, E.A., Longaker, M.T., Robbins, R.C., Wu, J.C. Patient-specific induced pluripotent stem cells as a model for familial dilated cardiomyopathy. *Science translational medicine*. 2012, 4:130ra147.

Takahashi-Yanaga, F., Morimoto, S., Harada, K., Minakami, R., Shiraishi, F., Ohta, M., Lu, Q.W., Sasaguri, T., Ohtsuki, I. Functional consequences of the mutations in human cardiac troponin I gene found in familial hypertrophic cardiomyopathy. *Journal of Molecular and Cellular Cardiology.* 2001, 33(12):2095-2107.

Takahashi-Yanaga, F., Morimoto, S., Ohtsuki, I. Effect of Arg145Gly mutation in human cardiac troponin I on the ATPase activity of cardiac myofibrils. *J Biochem*. 2000, 127(3):355-7.

Takahashi, M., Katagiri, T., Furuya, H., Hohjoh, H. Disease-causing allele-specific silencing against the ALK2 mutants, R206H and G356D, in fibrodysplasia ossificans progressiva. *Gene Ther.* 2012, 19(7):781-785.

Takeda, S., Yamashita, A., Maeda, K., Maéda, Y. Structure of the core domain of human cardiac troponin in the Ca (2+)-saturated form. *Nature*. 2003, 424(6944):35-41.

Tardiff, J.C., Hewett, T.E., Palmer, B.M., Olsson, C., Factor, S.M, Moore, R.L., Robbins, J., Leinwand, L.A. Cardiac troponin T mutations result in allele-specific phenotypes in a mouse model for hypertrophic cardiomyopathy. *J. Clin. Invest*. 1999, 104:469-481.

Tardiff, J.C. Thin filament mutations: developing an integrative approach to a complex disorder. *Circulation research.* 2011, 108: 765-782.

Theopistou, A., Anastasakis, A., Rigopoulos, A., Toutouzas, P., Stefanadis, C. Clinical features of hypertrophic cardiomyopathy caused by an Arg278Cys missense mutation in the cardiac troponin T gene. *Am J Cardiol.* 2004, 94(2):246-249.

Tobacman, L.S., Lin, D., Butters, C., Landis, C., Back, N., Pavlov, D., Homsher, E. Functional consequences of troponin T mutations found in hypertrophic cardiomyopathy. *J Biol Chem.* 1999, 274(40):28363-28370.

Toepfer, C.N., Wakimoto, H., Garfinkel, A.C., McDonough B, Liao, D., Jiang, J., Tai, A.C., Gorham, J.M., Lunde, I.G., Lun, M., Lynch, T.L., McNamara, J.W., Sadayappan, S., Redwood, C.S., Watkins, H.C., Seidman, J.G., Seidman, C.E. Hypertrophic cardiomyopathy mutations in MYBPC3 dysregulate myosin. *Sci Transl Med.* 2019, 11(476):eaat1199.

Towbin, J.A., Lowe, A.M., Colan, S.D., Sleeper, L.A., Orav, J., Clunie, S., Messere, J., Cox, G.F., Paul, R., Lurie, P.R., et al. Incidence, causes, and outcomes of dilated cardiomyopathy in children. *JAMA.* 2006, 296 1867-1876.

Townsend, P.J., Farza, H., Macgeoch, C., Spurr, N.K., Wade, R., Gahlmann, R., Yacoub, M.H., and Barton, P.J. Human cardiac troponin T: identification of fetal

isoforms and assignment of the TNNT2 locus to chromosome 1q. *Genomics.* 1994*,* 21(2):311-316.

Trochet, D., Prudhon, B., Beuvin, M., Peccate, C., Lorain, S., Julien, L., Benkhelifa-Ziyyat, S., Rabai, A., Mamchaoui, K., Ferry, A., Laporte, J., Guicheney, P., Vassilopoulos, S., Bitoun, M. Allele-specific silencing therapy for Dynamin 2-related dominant centronuclear myopathy. *EMBO Molecular Medicine*. 2018, 10(2):239-253.

Van der Velden, J., Tocchetti, C.G., Varricchi, G., Bianco, A., Sequeira, V., Hilfiker-Kleiner, D., Hamdani, N., Leite-Moreira, A.F., Mayr, M., Falcão-Pires, I., Thum, T., Dawson, D.K., Balligand, J.L., Heymans, S. Metabolic changes in hypertrophic cardiomyopathies: scientific update from the Working Group of Myocardial Function of the European Society of Cardiology. *Circulation Research*. 2018, 114(10):1273-1280.

Van Dijk, S.J., Dooijes, D., dos Remedios, C., Michels, M., Lamers, J.M., Winegrad, S., Schlossarek, S., Carrier, L., ten Cate, F.J., Stienen, G.J., van der Velden, J. Cardiac myosin-binding protein C mutations and hypertrophic cardiomyopathy: haploinsufficiency, deranged phosphorylation, and cardiomyocyte dysfunction. *Circulation.* 2009, 119:1473-1483.

Verma, I.M., Naldini, L., Kafti, T., et al. Gene therapy: promises, problems and prospects. *Nature.* 1997, 389(6648):239-42.

Walton, S.P., Wu, M., Gredell, J.A. and Chan, C. Designing highly active siRNAs for therapeutic applications. *FEBS J.* 2010, 277: 4806-4813.

Wang, L., Kim, K., Parikh, S., Cadar, A.G., Bersell, K.R., He, H., Pinto, J.R., Kryshtal, D.O., Knollmann, B.C. Hypertrophic cardiomyopathy-linked mutation in troponin T causes myofibrillar disarray and pro-arrhythmic action potential changes in human iPSC cardiomyocytes. *J Mol Cell Cardiol,* 2018, 114:320-327.

Wei, B., Jin, JP. Troponin T isoforms and posttranscriptional modifications: Evolution, regulation and function. *Archives of Biochemistry and Biophysics.* 2010, 505(2):144-154.

Willott, R.H., Gomes, A.V., Chang, A.N., Parvatiyar, M. S., Pinto, J.R., and Potter, J.D. Mutations in Troponin that cause HCM, DCM AND RCM: What can we learn about thin filament function? *J. Mol. Cell. Cardiol.* 2010, 48:882-892.

Xia, X.; Zhou, H.; Huang, Y.; Xu, Z. Allele-specific RNAi selectively silences mutant SOD1 and achieves significant therapeutic benefit in vivo. *Neurobiol. Dis*. 2006, 23:578–586.

Yanaga, F., Morimoto, S., Ohtsuki, I. Ca2+ sensitization and potentiation of the maximum level of myofibrillar ATPase activity caused by mutations of troponin T found in familial hypertrophic cardiomyopathy. *J Biol Chem*. 1999, 274 (13):8806-12.

Zhang, R., Zhao, J., Mandveno, A., Potter, J.D. Cardiac troponin I phosphorylation increases the rate of cardiac muscle relaxation. *Circulation research. 1995,* 76(6):1028-10.

Zot, A.S., Potter, J.D. Structural aspects of troponin-tropomyosin regulation of skeletal muscle contraction. *Annu Rev Biophys Biophys Chem.* 1987, 16:535-59.